# 55. A CD-Spectroscopic Alternative to Methylation Analysis of Oligosaccharides: Reference Spectra for Identification of Chromophoric Glycopyranoside Derivatives

by **William T. Wiesler, Nikolina Berova**[1]**, Makoto Ojika**[2]**, Harold V. Meyers**[3]**, Mayland Chang**[4]**, Peng Zhou, Lee-Chiang Lo, Masatake Niwa**[5]**, Reiji Takeda**[6]**,** and **Koji Nakanishi***

Department of Chemistry, Columbia University, New York, NY 10027, USA

(13.XII.89)

A microscale method for identifying the monosaccharide units and their linkages in oligosaccharides is presented. Sugar components are identified by UV and CD spectroscopy of chromophoric degradation products. CD spectral data for approximately 150 different glycopyranoside components are provided for use as reference spectra in the identification of unknown derivatives. Procedures for the conversion of oligosaccharides to monosaccharide subunits bearing 4-bromobenzoate and 4-methoxycinnamate chromophores have been developed based on acetolysis/bromination reactions for glycosidic cleavage of per(bromobenzoylated) oligosaccharides. The method offers an alternative means to conventional methylation analysis of oligosaccharides.

**1. Introduction.** – Recent years have seen a rapid growth in the understanding of the important and varied roles of oligosaccharides from glycoproteins and glycolipids [1]. These oligosaccharides play particularly important biological roles on cell surfaces and have been implicated as the antigenic determinants in a number of systems. Cell-cell recognition, cellular differentiation during development, and the attachment of viruses to cells during infection are all processes in which the cell-surface oligosaccharides are involved. Structurally diverse oligosaccharides are also constituents of other bioactive glycoconjugates such as saponins [2].

Determination of linkage structure in oligosaccharides has long relied upon methylation analysis by GLC/MS of partially methylated alditol acetates [3]. These monosaccharide residues are obtained by hydrolysis of permethylated oligosaccharides, reduction of the carbonyl group, and acetylation of the remaining OH groups which were originally involved in linkages. Methylation analysis generally requires a minimum of 25 nmol of material, although capillary GLC with smaller quantities have been reported [4]. The analysis relies heavily on chromatographic separation and comparison of monosaccharide derivative GLC retention times with a large bank of synthetic standards, few of which are commercially available. Linkage analysis generally follows a sugar-component

[1]) On leave from the Institute of Organic Chemistry, Bulgarian Academy of Sciences, BG-1113 Sofia.
[2]) Present address: Department of Chemistry, Faculty of Science, Nagoya University, Chikusa Nagoya 464, Japan.
[3]) Present address: *Vertex Pharmaceuticals, Inc.*, 40 Allston St., Cambridge, Mass. 02139, USA.
[4]) Present address: *Dow Chemical USA*, Agricultural Products Department, Midland, Michigan 48674, USA.
[5]) On leave from the Faculty of Pharmacy, Meijo University, Tempaku, Nagoya 468, Japan.
[6]) Present address: Suntory Institute for Bioorganic Research, Shimamoto, Mishima, Osaka, Japan.

analysis, and an additional analysis for determination of monosaccharide absolute configuration may be performed.

An alternative to methylation analysis based upon UV- and CD-spectroscopic analysis of HPLC-separated monosaccharide components bearing UV-active chromophores has been under development in our laboratories for several years [5–9]. The pursuit of this alternative methodology is justified by several important advantages which it offers over conventional methods. First, as a spectroscopic method, it does not rely on direct comparisons with synthetic standards and, thus, would be more accessible to non-specialists in fields outside of carbohydrate chemistry; instead, monosaccharide components are identified by CD, a widely used and readily available technique in biology and biochemistry. Second, only nanomole quantities of chromophorically modified sugar components are required for CD measurements, and these spectra are compared with the 150 reference CD data given below. Finally, CD spectra provide more structural information than that obtained by methylation analysis. In most cases, the CD spectra indicate the identity of the component monosaccharide, its linkage pattern, and its absolute configuration. Low-resolution (LR) MS and HPLC retention time provide additional information regarding the presence of various functional groups such as AcN, BzN, AcO, or the absence of O-functions (deoxy sugars).

Recent CD studies have shown that the CD spectra of glycopyranosides bearing a combination of 4-bromobenzoate ($\lambda_{max}$ 245 nm) and 4-methoxycinnamate ($\lambda_{max}$ 311 nm) chromophores are characteristic for each type of monosaccharide and substitution pattern [9–12]. Therefore, we envisioned, using these two different exciton-coupling chromophores, to selectively tag free OH groups and those originally involved in glycosidic linkages (see *Scheme 1*). By simple analogy to methylation analysis, this roughly corresponds to using the 4-bromobenzoate chromophores in place of the Me groups of methylation analysis, and 4-methoxycinnamate chromophores instead of acetates to tag OH groups liberated from glycosidic linkages. Degradation of oligosaccharides with the selective introduction of these chromophores can be achieved by a variety of procedures. The resulting UV-active monosaccharide subunits are then separated by HPLC and subjected to UV, CD, and MS analysis. The ratio of the two chromophores present are readily determined by UV, thus indicating the number of other sugar residues to which the particular sugar was linked; the CD spectra of the individual components serve to identify the monosaccharides *and* their chromophore substitution patterns, the latter representing the linkage patterns of each monosaccharide component in the original oligosaccharide. After UV and CD analysis, samples are subjected to MS for further structural analysis if necessary.

We present here a complete CD spectral library for the identification of many types of glycopyranoside components obtainable from oligosaccharides. The CD data base is presently restricted to pyranoside components, as CD calculations are not straightforward for the conformationally flexible furanosides (see [13], p. 143–145). Thus, spectral data for furanoside components must be obtained experimentally, after which it can be used for comparison purposes. The utility of the glycopyranoside spectra is demonstrated by a number of model studies in which known oligosaccharides have been transformed to the appropriate chromophoric monosaccharide subunits for spectral analysis. Procedures for the formation of the required derivatives, based upon a novel glycosidic cleavage, are presented and shown to be applicable on a nanomole scale.

*Scheme 1*

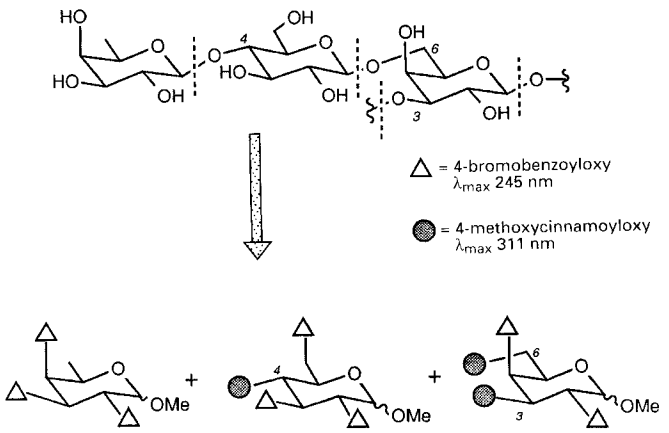


**2. Formation of the Required Monosaccharide Derivatives.** – Preliminary efforts to obtain bichromophoric derivatives[7]) of the type shown in *Scheme 1* involved an initial peralkylation of oligosaccharides with either benzyl or allyl protecting groups. Glycosidic linkages in the peralkylated oligosaccharides were subsequently cleaved under methanolysis conditions using a *Teflon* bomb in a microwave oven. The mixture of cleavage products was then per(bromobenzoylated) (tagging linkage OH groups), deprotected, and finally methoxycinnamoylated (tagging originally free OH groups). When the benzyl protecting group was used, deprotection/methoxycinnamoylation could be achieved in a single pot in high yields[8]). However, several drawbacks made the five-step sequence unattractive, and it remained difficult to carry out this procedure on submilligram quantities.

A more straightforward approach to bichromophoric monosaccharide derivatives involved the direct cleavage of per(bromobenzoylated) oligosaccharides, thus eliminating protection/deprotection steps; importantly, per(bromobenzoates) could be prepared in high yields, and furthermore, their lipophilic properties greatly facilitated purification by HPLC when the starting oligosaccharide was contaminated. While methanolysis of per(bromobenzoylated) oligosaccharides was found to be sluggish and to result in undesired acyl migration or ester hydrolysis, acetolysis/bromination conditions (AcOH/HBr/AcBr) [14] were found to be ideally suited for degradation of per(bromobenzoylated) oligosaccharides [15]. We have developed two variations of the acetolysis/bromination reaction which are suitable for oligosaccharide per(bromobenzoates).

---

[7]) In earlier studies, only a single chromophore was used that resists conventional glycosidic-cleavage conditions, the 4-phenylbenzyloxy group ($\lambda_{max}$ 253 nm), to tag the free OH groups; the substitution pattern was then derived from the amplitudes of the exciton-split curve [5–9]. However, this monochromophoric approach suffers from the low per(phenylbenzylation) yield, difficulty in cleavage of glycosidic linkages, and the necessity for identifying the sugar units separately.

[8]) The oligosaccharide was perbenzylated; then, the glycosidic bonds were cleaved by methanolysis in a microwave oven, the liberated OH groups bromobenzoylated, and the benzylated groups converted into 4-methoxycinnamates by a one-pot microreaction (90%) consisting of two steps: treatment with $FeCl_3$/$CH_2Cl_2$ at r.t. for 1 h [8] and then with 4-MeOCnCl/AgOTf/pyridine at r.t. for 1 h (*M. Chang*, unpublished).

Due to the large number of monosaccharide derivatives discussed in this paper, *the chromophoric methyl glycopyranosides are represented by the short form of the corresponding glycose followed by a four-symbol descriptor to designate the substituents at positions 2, 3, 4, and 6 of the methyl glycopyranoside* (2, 3, 4 for a pentopyranoside or 6-deoxyhexopyranoside), *their sequence corresponding to the above order of locants;* for convenience, configurational symbols are omitted: *O* = free OH group, Ac = *O*-acetyl, (BrAc) = *O*-bromoacetyl, *B* = *O*-(4-bromobenzoyl), *C* = *O*-(4-methoxycinnamoyl) and N*B* = *N*-(4-bromobenzoyl); *e.g.*, Glc*BBCC* denotes (D-configurated) methyl glucopyranoside 2,3-bis(4-bromobenzoate) 4,6-bis(4-methoxycinnamate).

2.1. *Trifluoroacetolysis/Bromination* (see *Scheme 2*). Acetolysis/bromination conditions (HBr in AcOH) applied to lactose octakis(4-bromobenzoate) were found to effect glycosidic cleavage with concomitant acetylation of the linkage OH groups where intro-

*Scheme 2*

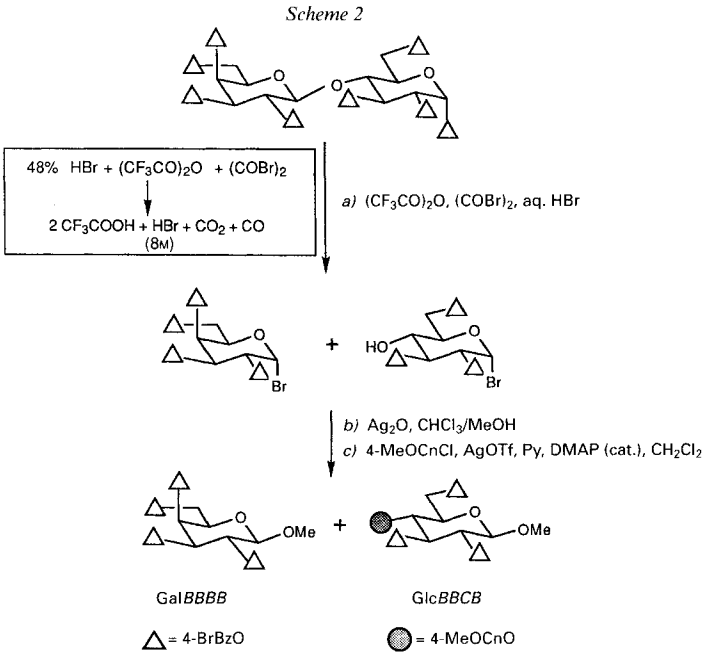


duction of the 4-methoxycinnamate chromophore is desired. While AcO groups are not readily removable in the presence of bromobenzoates, a variety of haloacetates can be deprotected and replaced with the second chromophore.

The $CF_3COO$ group represents one type of labile acetate and thus, the acetolysis/bromination was tried in $CF_3COOH$ as solvent. Anhydrous 8M HBr/$CF_3COOH$ was generated by combining 48% aq. HBr solution with $(CF_3CO)_2O$ and oxalyl bromide (41:79:130 *v/v*) [9]. Treatment of lactose octakis(4-bromobenzoate) with this reagent for 30 min at 100° in a sealed tube[9]) afforded two glycosyl bromides (derivatives of Gal*BBBB*

[9]) *Caution*: as CO, $CO_2$, and HBr are liberated from oxalyl bromide during the cleavage reaction, dangerous pressures may be generated. However, the reactions can be safely carried out in the heavy-glass vessels utilized in these studies (see *Fig. 1a, Footnote 10*, below).

and Glc*BBOB*), one bearing a free OH group at the linkage position (*Scheme 2*). The transient presence of a $CF_3CO$ at the OH group involved in the glycosidic linkage, which is presumably lost during workup, accounts for the absence of acyl-migration products. Addition of stoichiometric amounts of $H_2O$ to varying ratios of $(CF_3CO)_2O$ and $(COBr)_2$ enabled manipulation of the HBr concentration; an 8M HBr/$CF_3COOH$ solution was optimal for clean, complete cleavage reactions. After removal of HBr (gas) and $CF_3COOH$ under reduced pressure, the glycosyl bromides were converted to their methyl glycosides with MeOH/$Ag_2O$. Methoxycinnamoylation of the mixture with 4-methoxycinnamoyl chloride (4-MeOCnCl) in the presence of silver trifluoromethanesulfonate (AgOTf) and 4-(dimethylamino)pyridine (DMAP) in pyridine (Py)/$CH_2Cl_2$ gave then Gal*BBBB* and Glc*BBCB*, the CD curves of which agreed well with synthetically prepared standards. This three-step reaction sequence was similarly applied with success to stachyose tetradecakis(4-bromobenzoate) and stevioside undecakis(4-bromobenzoate) [9]. However, application to oligosaccharides containing deoxyglycopyranose (*e.g.*, quinovose = 6-deoxyglucose), pentopyranose (*e.g.*, xylose, arabinose), branched hexopyranose and aminodeoxysugars gave multiple decomposition products, thus limiting the utility of these cleavage conditions.

2.2. *Bromoacetolysis/Bromination* (see *Scheme 3*). A cleavage reaction amenable to hexopyranoses and deoxysugars, including branched sugars and aminodeoxysugars, was uncovered, when $CF_3COOH$ was replaced with $BrCH_2COOH$ [15]. It is summarized in *Scheme 3*.

2.2.1. *Cleavage of Glycosidic Bond.* $BrCH_2COBr/H_2O$ mixtures were found to cleave glycosidic linkages in per(bromobenzoylated) oligosaccharides with concomitant protec-

*Scheme 3*

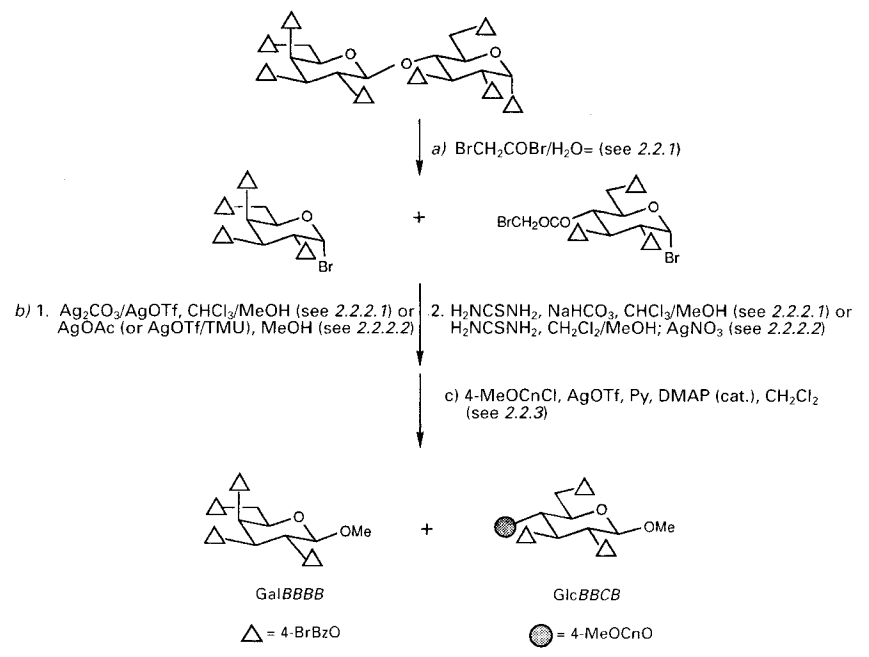

tion of liberated OH groups as bromoacetates *(Scheme 3)*. Thus, bromobenzoyl migration was prevented and the integrity of the linkage points maintained. Cleavage reactions were conveniently performed in glass tubes (1.1- or 3.3-ml capacity) fitted with *Teflon* screw caps[10]) to confine HBr during the reactions. Optimal utilization of the $BrCH_2COBr/H_2O$ reagent required varying both time and temperature of the cleavage reaction. Cleavage rates were dependent upon the particular sugars and linkages. In general, β-D linkages were cleaved more readily than α-D linkages. Terminal and 6-linked sugar residues were most rapidly cleaved, followed by 3-linked residues; 2- and 4-linked residues were the most difficult to liberate. This is consistent with observed rates of acetolysis for pyranose-containing dissacharides [16].

The $BrCH_2COOH$ formed by the cleavage reaction was removed by $NaHCO_3$ workup, and this was followed by application of *Procedure 2.2.2.1* as described below for digitonin (see *Scheme 4* and *Exper. Part*). However, in the case of *N*-acetylated 2-amino-2-deoxysugars, the $NaHCO_3$ workup was deleted because this step led to partial decomposition of the unstable intermediate glycosyl bromides; as described below for sarasinoside $C_1$ (see *Scheme 5* and *Exper. Part*), the crude cleavage product was submitted in these cases to *Procedure 2.2.2.2.*

2.2.2. *Conversion of α-D-Glycopyranosyl Bromides to Methyl β-D-Glycopyranosides and Removal of Bromoacetyl Group(s).* 2.2.2.1. *Oligosaccharides without N-Acetylated 2-Amino-2-deoxy Sugars.* After removal of $BrCH_2COOH$ with aq. $NaHCO_3$ solution, the mixture was immediately converted to stable methyl β-D-glycosides with $Ag_2CO_3/AgOTf$ in $MeOH/CHCl_3$ *(Scheme 3)*. Removal of bromoacetyl groups with thiourea[11]) [17] yielded the mixture of the desired methyl β-D-glycopyranosides.

2.2.2.2. *More General Conditions.* They differ only slightly from those described in *2.2.2.1* in the sense that the glycosyl bromides were converted into the methyl glycosides in the presence of $BrCH_2COOH$ with AgOAc or AgOTf/tetramethylurea (TMU) rather than with $Ag_2O$ (see *Scheme 2*) or $Ag_2CO_3$ *(Scheme 3)*. The use of $Ag_2O$ or $Ag_2CO_3$ in the glycosidation step leds to hydrolysis products (*i.e.*, δ-lactol formation), because $H_2O$ was generated from these silver reagents in the presence of $BrCH_2COOH$[12]). Workup was facilitated by addition of $AgNO_3$ to precipitate the thiourea which coeluted with some aminodeoxysugars on silica gel.

2.2.3. *Methoxycinnamoylation.* Free OH groups involved in glycosidic linkages were methoxycinnamoylated in high yield using the conditions described in *Chapt. 2.1 (Scheme 3)*.

Lactose octakis(4-bromobenzoate) was subjected to this cleavage and conversion sequence to provide the same chromophoric products as obtained using the trifluoroacetolysis/bromination approach (see *Chapt. 2.1* and *Scheme 2*). The four-step sequence in *Scheme 3* is efficient and convenient, as purification is required only after the final step to separate the subunits for spectroscopic analysis.

---

[10]) Excellent reaction tubes for these high-pressure reactions are conveniently prepared from high-vacuum valves *(Teflon, Kontes)* by cutting and sealing the bottom and side-arm (see *Fig. 1a*, below).

[11]) Aminoethanethiol hydrochloride/$NaHCO_3$ (excess) in $MeOH/CHCl_3$ can also be used to effect bromoacetyl removal.

[12]) Mercury salts (*e.g.*, $Hg(CN)_2/HgBr_2$) were also successfully employed to effect glycosidation, but they were difficult to remove afterwards.

*Scheme 4*

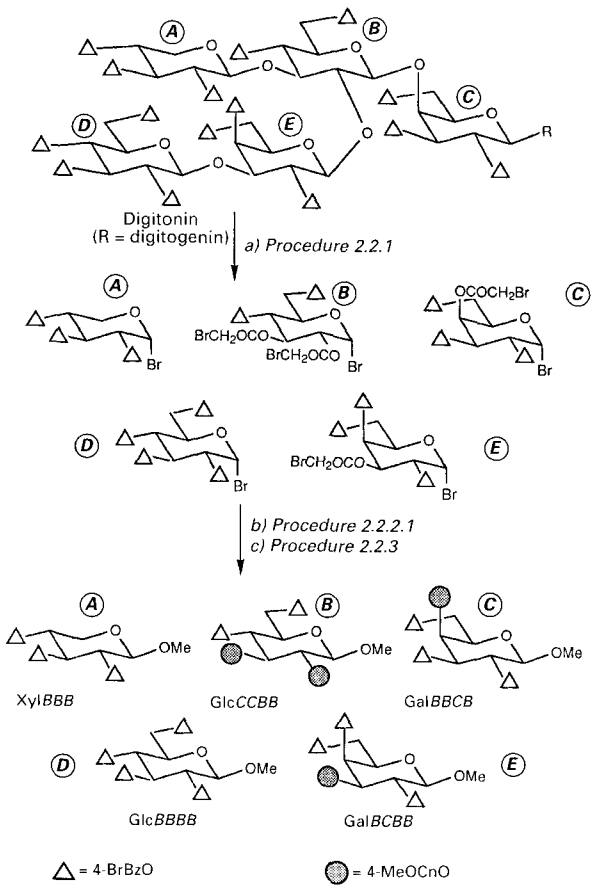


**3. Applications.** – The earlier version of the general procedure, described in *2.2.1*, *2.2.2.1*, and *2.2.3*, was applied to digitonin heptadecakis(4-bromobenzoate) *(Scheme 4)* [15]. Treatment of this heptadecakis(4-bromobenzoate) (300 μg, 70 nmol) in $BrCH_2COBr/H_2O$ (1:1 molar ratio, which generates a 9.5M HBr/$BrCH_2COOH$ solution) for 12 h at 60° gave the α-D-glycosyl bromides corresponding to Xyl*BBB* (Ⓐ), Glc(BrAc)$_2$*BB* (Ⓑ), Gal*BB*(BrAc)*B* (Ⓒ), Glc*BBBB* (Ⓓ), and Gal*B*(BrAc)*BB* (Ⓔ). After glycosidation, removal of bromoacetyl groups with thiourea, and subsequent methoxycinnamoylation, the bichromophoric mixture of Xyl*BBB*, Glc*CCBB*, Gal*BBCB*, Glc*BBBB*, and Gal*BCBB* was obtained, in 41, 69, 31, 94, and 35% overall yield, respectively[13]). The resulting degradation products were separated by HPLC (*Fig. 1b*) and characterized by CD *(Fig. 1c–g)*. As can be seen in *Fig. 1*, excellent agreement was found between CD spectra of these components and synthetic standards which had been previously prepared [5] [6] [9].

[13]) Yields of the HPLC-separated components were determined by UV. Concentrations of each in a given volume of MeCN were calculated using the previously determined extinction coefficients (see *Exper. Part*).

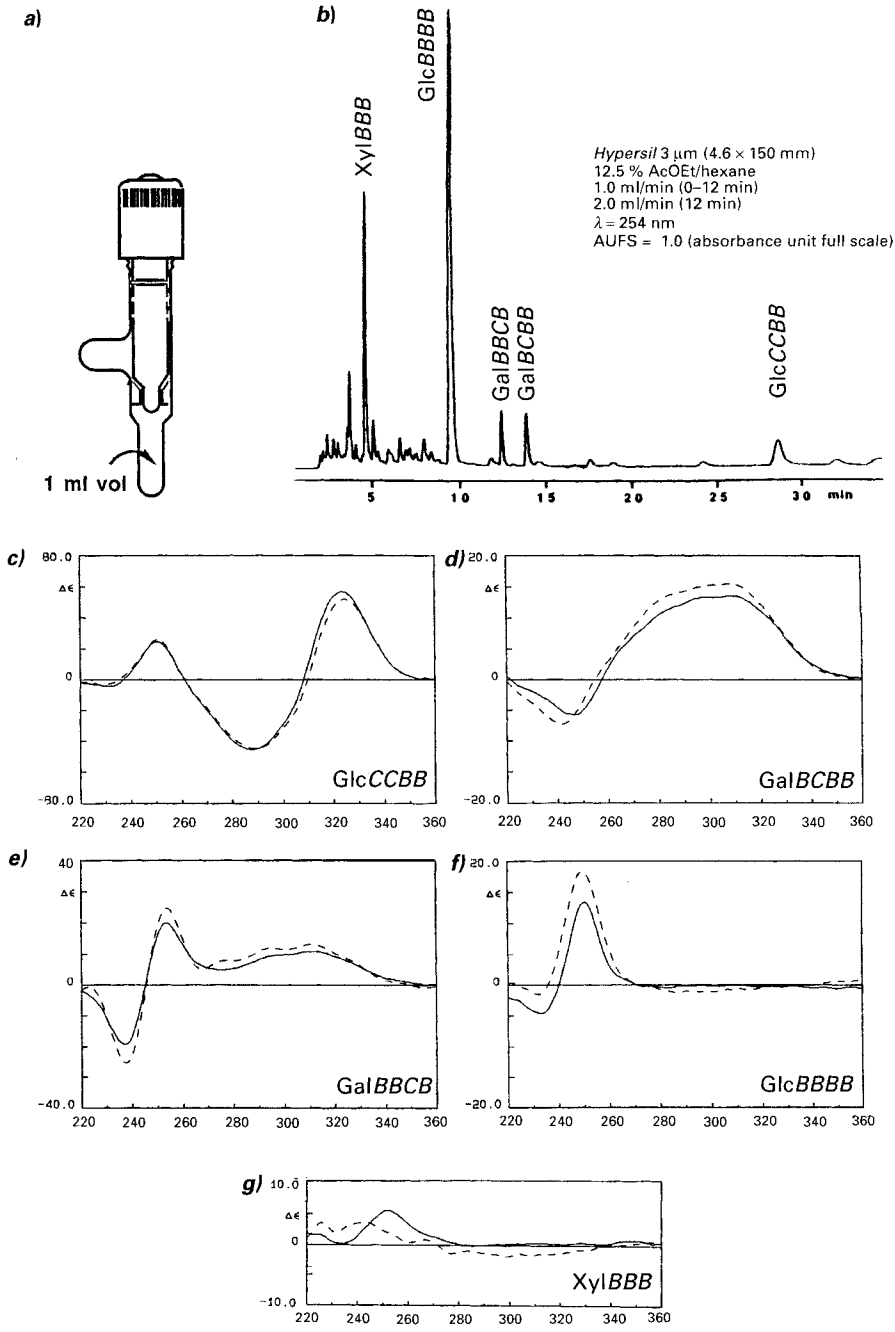


Fig. 1. a) *Bromoacetolysis/Brominoation-reaction tube*; b) *HPLC and* c)–g) *CD spectra of products obtained from digitonin* (solid line; β-D-configuration) *compared with authentic materials* (c–f, dotted line) *or with data calculated for the corresponding* α-D-*glycoside* (g, dotted line)

*Scheme 5*

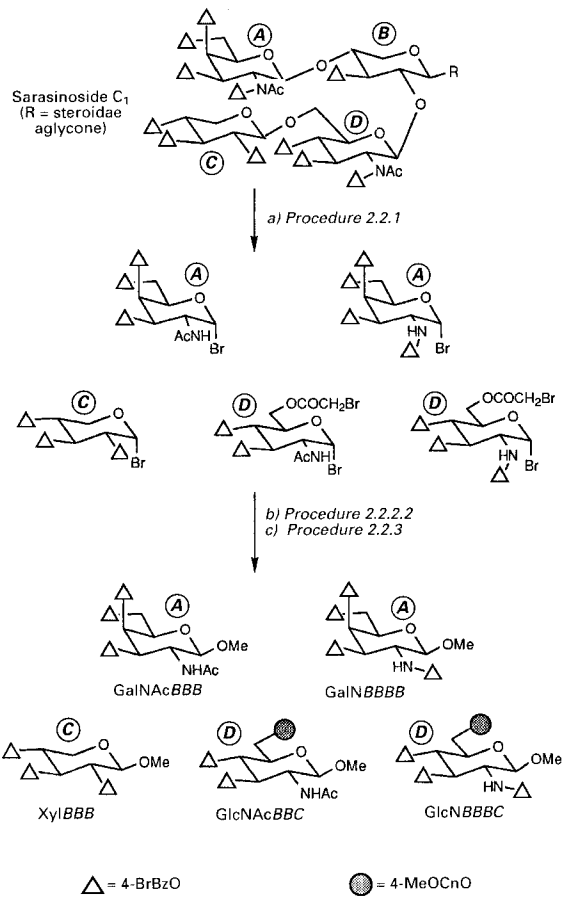


As mentioned above, the more general method *2.2.2.2* was for oligosaccharides containing *N*-acetylated aminodeoxysugars. Their bromobenzoylation under standard conditions produced varying amounts of *N*-diacylated products. *E.g.*, bromobenzoylation of sarasinoside $C_1$ (260 µg, 95 nmol; *Scheme 5*) resulted in complete *N*-bromobenzoylation to give the undecakis(4-bromobenzoate). Cleavage with stoichiometric amounts of $BrCH_2COBr/H_2O$ (83 µl/17 µl; 50°, 12 h) followed by glycosidation with AgOTf/TMU in MeOH, deprotection, and methoxycinnamoylation yielded five major products separated by HPLC[14]) *(Fig. 2)*. Each *N*-acetylated aminodeoxysugar moiety was found to give rise to two products, an *N*-acetylated and an *N*-benzoylated derivative. During the glycosidic cleavage, loss of the *N*-acetyl group predominated over that of the *N*-benzoyl group, providing GalN*BBBB* and GlcN*BBBC* as major products and GalNAc*BBB* and GlcNAc*BBC* as minor products. Similar cleavage results were obtained

[14]) Cleavage with stoichiometric amounts of $BrCH_2COBr$ (158 µl, 1.8 mmol) and 48% aq. HBr solution (42 µl; 0.37 mmol HBr and 1.8 mmol $H_2O$) for 12 h at 42° gave similar results.

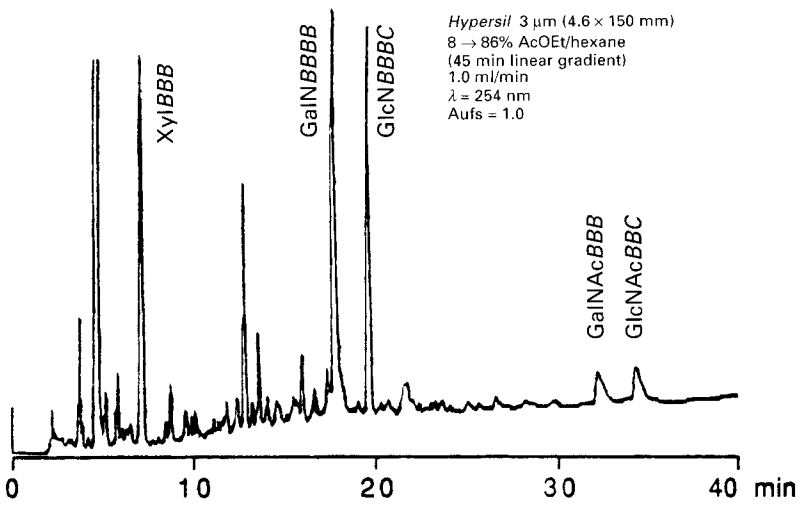


Fig. 2. *HPLC profile of products obtained from sarasinoside C using gradient elution*

with $BrCH_2COBr/H_2O$ (103 µl/17 µl, 1:0.8 molar ratio; 60°, 4 h). The unstable, branched xylopyranose Ⓑ was not observed under any conditions[15]). The terminal xylopyranose Ⓒ, however, provided the expected Xyl*BBB*. Higher cleavage temperatures and longer reaction times (*e.g.*, 60°, 24 h) led to decomposition of the terminal xylose residue, while lower temperatures (*e.g.*, r.t., 70 h) appeared to effect partial cleavage with stoichiometric amounts of $BrCH_2COBr/H_2O$.

A variety of model disaccharides and saponins bearing *N*-acetylated aminodeoxysugars have been examined with satisfactory results[16]). However, certain cases were consistently prone to either decomposition or rearrangement. For example, 3- and 4-linked GlcNAc residues typically yielded the expected cleavage products, while 3- and 4-linked GalNAc residues were more problematic; 4-linked GalNAc residues gave rise to a single rearrangement product, an *N*-acetylated methyl 2-amino-2-deoxyglycofuranoside. The 2-(acetamido)glycosyl bromides were found to be particularly sensitive to hydrolysis, making it important to maintain anhydrous conditions in the cleavage procedure. Studies are ongoing to improve and develop the methodology for the conversion to the required monosaccharide derivatives and, in particular, for the cleavage reaction, balancing the need to effect complete glycosidic cleavage on the one hand, while preventing decomposition of less stable sugar residues, including mannose, on the other.

**4. HPLC Separation of the Monosaccharide Derivatives.** – AcOEt/hexane solvent systems and a 3-µm *Hypersil* analytical column were used throughout these studies. AcOEt/hexane 1:4 was sufficient for separation of simple two-component mixtures

[15]) Synthetic methyl β-D-xylopyranoside 3-(4-bromobenzoate) 2,4-bis(bromoacetate) was co-injected with the cleavage mixture after the glycosidation step to confirm the absence of this expected cleavage product.

[16]) Best results were obtained on model disaccharides containing *N*-acetylated aminodeoxysugars when a slight excess of $BrCH_2COBr$ over $H_2O$ was employed (1:0.8).

obtained from disaccharides such as lactose, while a less polar system (AcOEt/hexane 1:7) was required for separation of residues obtained from digitonin. As seen above in *Fig. 1b*, the presence of 4-methoxycinnamoyl groups *(C)* results in longer retention times than the presence of 4-bromobenzoyl groups *(B)*. Thus, tris- and tetrakis(4-bromobenzoates) ($B_3$ and $B_4$, resp.) elute from the column first, followed by tris(4-bromobenzoate) mono(4-methoxycinnamates) ($B_3C$) and then bis(4-bromobenzoate) bis(4-methoxycinnamates) ($B_2C_2$). Analogously, mono(4-bromobenzoate) tris(4-methoxycinnamates) ($BC_3$) would follow.

A second important determinant of HPLC elution order is the presence of aminodeoxysugars, which require the use of gradient solvent systems because of their increased polarity. Thus, for all studies involving *N*-acylated aminodeoxysugars, a 45-min linear gradient from 8 to 86% AcOEt/hexane was employed. As seen in *Fig. 2*, *N*-benzoylated aminodeoxysugars elute before the corresponding *N*-acetylated aminodeoxysugars. While this type of gradient system provides good separation between different types of sugar derivatives, it may not provide good separation between structural isomers of similar polarity. More complex component mixtures may require an initial gradient separation followed by one or more separations with isocratic solvent systems which are better suited to separate derivatives with similar substituents (*e.g.*, Gal*BBCB* and Gal*BCBB*, as shown in *Fig. 1b*).

In conventional methylation analysis, structural assignments rest to a large degree upon comparison of GLC retention times. In the spectroscopic approach presented here, the HPLC retention time data can serve to supplement the spectral data. As more derivatives are examined, the elution profiles of these products can be catalogued and used to confirm structural assignments.

**5. UV Spectral Analysis of the Monosaccharide Derivatives.** – After isolation of the sugar derivatives from HPLC, they were analysed by UV in the range of 200–400 nm. HPLC retention times provided some indication of the type of sugar (such as aminodeoxysugar) and the types of chromophores present. The ratio of 4-bromobenzoate to 4-methoxycinnamate chromophores was determined by a simple analysis of UV spectra *(Table 1)*.

Derivatives obtained from terminal sugar subunits have only 4-bromobenzoate chromophores with an absorption maximum at 245 nm ($A_{245}$) and, essentially, transparency above 300 nm. Products derived from sugars having a single linkage point again have an

Table 1. *Classification of Monosaccaride Derivatives by UV Absorbance Ratios*

| Class[a]) | $A_{245}/A_{310}$[b]) | CD Data | Linkage type |
|---|---|---|---|
| $B_n$ | $\infty$ | *Table 2* | terminal |
| $B_3C$ | *ca.* 2.8 | *Figs. 4–5 (Spectra 1–12)* | single linkage |
| $B_2C$ | *ca.* 1.5 | *Figs. 11–17 (Spectra 43–84)* | single linkage |
| $B_2C_2$ | 0.8–1.0 | *Figs. 8–10 (Spectra 25–42)* | branching |
| $BC_2$ | 0.42–0.57 | *Figs. 18–24 (Spectra 85–126)* | branching |
| $BC_3$ | 0.30–0.43 | *Figs. 6–7 (Spectra 13–24)* | 3-way branching |

[a]) *B* = 4-Bromobenzoyl group, *C* = 4-methoxycinnamoyl group.
[b]) Absorbance at 245 and 310 nm, resp.

absorption maximum at 245 nm in addition to a second, smaller 4-methoxycinnamate absorption at 310 nm ($A_{310}$). In products derived from branching sugars having two or three linkages, the 310-nm 4-methoxycinnamate absorption is greater or roughly equal to the 4-bromobenzoate absorption at 245 nm. The ratio of absorbances $A_{245}/A_{310}$ has been quantified for a number of derivatives having combinations of three or four chromophores (see *Table 1*). A discrete range of ratios is observed for each class of compounds. For the mono(4-bromobenzoate) bis- and tris(4-methoxycinnamates) ($BC_2$ and $BC_3$), overlapping of observed ratios at values 0.42–0.43 leads to some ambiguity. However, the $BC_3$ derivatives are only expected from infrequently occurring sugar components which have three linkage points. Ambiguities can be resolved by subjecting the product to MS following CD analysis.

While not necessary in all cases, mass spectra must be obtained for monosaccharide derivatives having only 4-bromobenzoate chromophores as indicated by UV since the UV provides no indication of the number of *B* groups present which is crucial to the CD analysis. Low-resolution MS can easily indicate the number of *B* groups and the types of functional groups present. *E.g.*, 6-deoxyhexopyranoside and pentopyranoside derivatives having similar HPLC, UV, and CD can only be distinguished by MS.

**6. Circular Dichroism Data Base.** – In our ongoing CD studies of bichromophoric sugar derivatives [10–12], we have found that derivatives bearing 4-bromobenzoate and 4-methoxycinnamate chromophores have highly characteristic CD spectra which are in accord with the principles of exciton coupling [13]. The accumulated data base currently consists of roughly 60 spectra of tri- and tetrachromophoric glycopyranosides and another 72 spectra of dichromophoric glycopyranosides, all of which have been prepared synthetically. Another 12 spectra of tri- or tetrachromophoric monosaccharide derivatives obtained by conversion of oligosaccharides completes the inventory at this time. The 72 dichromophoric derivatives are all the possible permutational isomers of methyl α-D-gluco-, galacto-, and mannopyranoside bearing two chromophores (4-bromobenzoates, 4-methoxycinnamates, or one of each) and two acetyl groups. The CD spectra of these 72 dichromophoric glycopyranosides represent the spectral contributions of all possible pairwise interactions which contribute to the spectra of tri- and tetrachromophoric derivatives in an additive fashion. These 72 spectra are referred to as the 'basis set', because they can be algebraically summed to provide simulated spectra of tri- and tetrachromophoric derivatives.

The 72 previously reported basis-set spectra [10–12] have been digitally smoothed in this paper to improve the signal/noise ratio and have been used to calculate CD curves for all possible tri- and tetrachromophoric pyranoside derivatives related to the glucose, galactose, and mannose parent sugars. The calculation procedure involves algebraic summation of either the three (for trichromophoric derivatives) or six (for tetrachromophoric derivatives) basis-set spectra which represent the constituent pairwise two-chromophore interactions in the tri- and tetrachromophoric derivatives in question. *E.g.*, *Fig. 3* shows the six basis-set spectra corresponding to each of the six pairwise interactions in methyl galactopyranoside 3-(4-bromobenzoate) 2,4,6-tris(4-methoxycinnamate) (Gal*CBCC*). These include three spectra for *B*/*C* interactions (**I–III**) and three for *C*(*C* interactions (**IV–VI**). *B*/*C* interactions give rise to *Cotton* effects around the absorption maxima of the two chromophores (245 and 311 nm) and *C*/*C* interactions to two *Cotton* effects centered around the *C*absorption maximum at 311 nm[17]). The sum of

[17]) While none are present in this example, *B*/*B* interactions give rise to two *Cotton* effects around 245 nm (see, *e.g.*, CD spectra of Glc*BBBB* and Xyl*BBB*, *Fig. 1f* and *g*).

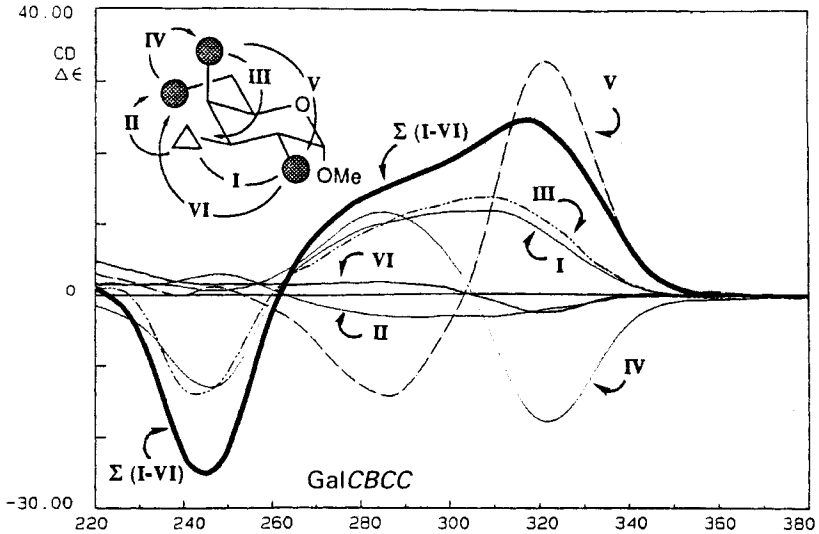


Fig. 3. *CD curves of the six basis-set derivatives* **I**–**VI** *and their sum for Gal*CBCC. ● = 4-Bromobenzoyloxy (*B*O), △ = 4-methoxycinnamoyloxy (*C*O). **I** = Gal*CB*AcAc, **II** = GalAc*B*Ac*C*, **III** = GalAc*BC*Ac, **IV** = GalAcAc*CC*, **V** = Gal*C*Ac*C*Ac, **VI** = Gal*C*AcAc*C*.

these six spectra provides a satisfactory simulation of Gal*CBCC* (see *Fig. 6, Spectrum 16*, for a comparison of calculated *vs.* observed CD's).

Calculated data for tris- and tetrakis(4-bromobenzoates) are presented in *Table 2* and in *Figs. 4–24* together with observed spectra from authentic samples obtained synthetically or by conversion of commercially available di-, tri-, or tetrasaccharides. In *Figs. 4–24*, the *spectrum calculated for the derivative given at the bottom right* (no configurational symbol means D) is depicted by the *solid line* (——). *Observed spectra are presented by broken* (– – –; synthetic authentic sample) and *broken dotted lines* (– · – · –; product isolated after cleavage, *i.e.* oligosaccharide-conversion product). The agreement between calculated and observed spectra is very good for all except a few cases[18]). Naturally, experimental curves are the reference spectra of choice, and we are continuing to expand the experimental data base. Calculated spectra can also be used as reference spectra with a reasonable degree of confidence, but care should be taken to consider alternative structures which have closely related spectra. Inversion of configuration at the anomeric center gives rise to only small differences in CD curves [11]. While the current oligosaccharide-conversion procedures yield methyl β-D- or β-L-glycosides for glucose and galactose, and α-D-glycosides for mannose [12], most of the synthetic standards have been prepared from the methyl α-D- or α-L-anomer. A number

[18]) Discrepancies are observed in some glucose derivatives where the calculated spectra are very weak. In such cases, the three equatorial chromophores at C(2), C(3), and C(4) adopt a nearly symmetrical orientation with respect to the pyranoside ring. Equal pairwise interactions of opposite signs result in a weak net spectrum, making deviations arising from conformational differences about the C(5)–C(6) bond [8] and other effects more pronounced. See, *e.g.*, Glc*BCBB* (*Fig. 4, Spectrum 6*) and Glc*CBCC* (*Fig. 6, Spectrum 18*).

Table 2. *Calculated and Observed CD Data for Methyl Glycopyranoside Tetrakis- and Tris(4-bromobenzoates)*

| *Entry* | Compound | Calc. CD [a]) | $A_{calc.}$ [b]) | Obs. CD[c]) | $A_{obs.}$ [b]) |
|---|---|---|---|---|---|
| *1* | α-D-Glc*BBBB* | 225 (+10), 250 (+31) | – | 221 (+2), 249 (+20) | – |
| *2* | β-D-Glc*BBBB* | 225 (+10), 250 (+31) | – | 233 (−7), 251 (+25) | +32 |
| *3* | α-D-Gal*BBBB* | 234 (−18), 252 (+95) | +113 | 237 (−29), 253 (+70) | +99[d]) |
| *4* | α-D-GalN*BBBB* | 234 (−18), 252 (+95) | +113 | 237 (−27), 252 (+71) | +98[c]) |
| *5* | β-D-Gal*BBBB* | 234 (−18), 252 (+95) | +113 | 237 (−26), 252 (+74) | +100[d]) |
| *6* | α-D-Man*BBBB* | 234 (+26), 252 (−82) | −108 | 237 (+23), 252 (−66) | −89[e]) |
| *7* | α-D-Glc*BBB*Ac | 226 (+4), 243 (+4) | – | | |
| *8* | β-D-Xyl*BBB* | 226 (+4), 243 (+4) | – | 235 (−3), 251 (+7) | +10 |
| *9* | β-D-Vio*BBB*[f]) | 226 (+4), 243 (+4) | – | 237 (−6), 253 (+11) | +17 |
| *10* | α-D-Gal*BBB*Ac | 233 (−30), 252 (+119) | +149 | 236 (−42), 253 (+95) | +137[d]) |
| *11* | β-L-Ara*BBB* | 233 (−30), 252 (+119) | +149 | 236 (−32), 253 (+101) | +133[d]) |
| *12* | α-L-Gal*BBB*Ac | 233 (+30), 252 (−119) | −149 | – | – |
| *13* | α-L-Fuc*BBB* | 233 (+30), 252 (−119) | −149 | 236 (+30), 252 (−100) | −130[c]) |
| *14* | β-L-Fuc*BBB* | 233 (+30), 252 (−119) | −149 | 233 (+29), 251 (−99) | −128 |
| *15* | α-L-Man*BBB*Ac | 234 (−28), 252 (+103) | +131 | – | – |
| *16* | α-L-Rha*BBB* | 234 (−28), 252 (+103) | +131 | 237 (−30), 252 (+101) | +131[c]) |
| *17* | α-D-Glc*BB*Ac*B* | 234 (−14), 252 (+54) | +68 | 236 (−22), 253 (+47) | +69[d]) |
| *18* | α-D-Gal*BB*Ac*B* | 234 (−15), 253 (+40) | +55 | 234 (−14), 253 (+31) | +45[d]) |
| *19* | β-D-Gal*BB*Ac*B* | 234 (−15), 253 (+40) | +55 | 236 (−16), 253 (+30) | +46[d]) |
| *20* | α-D-Man*BB*Ac*B* | 229 (+8), 252 (−31) | −39 | – | – |
| *21* | α-D-Glc*B*Ac*BB* | 247 (+14) | – | 236 (−), 253 (+8) | +9[d]) |
| *22* | α-D-Gal*B*Ac*BB* | 233 (+7), 249 (+13) | – | 253 (+6) | – |
| *23* | α-D-Man*B*Ac*BB* | 221 (+2), 250 (−11) | – | – | – |
| *24* | α-D-GlcAc*BBB* | 239 (+16), 252 (−12) | −28 | 236 (+11), 253 (−22) | −33[d]) |
| *25* | β-D-Glc*OBBB* | 239 (+16), 252 (−12) | −28 | 236 (+11), 253 (−19) | −30 |
| *26* | β-D-GlcAc*BBB* | 239 (+16), 252 (−12) | −28 | 236 (+8), 254 (−18) | −26 |
| *27* | α-D-GalAc*BBB* | 229 (+4), 253 (+16) | – | – | – |
| *28* | β-D-GalNAc*BBB* | 229 (+4), 253 (+16) | – | 227 (+3), 254 (+10) | – |
| *29* | α-D-ManAc*BBB* | 237 (+19), 253 (−20) | −39 | – | – |

[a]) Calculated CD by summation of corresponding pairwise interactions from the homo basis set (wavelength in nm ($\Delta\varepsilon$)).

[b]) 'Amplitude' or difference in $\Delta\varepsilon$ values of the two extrema of exciton-split CD curves (see [13]).

[c]) Experimentally measured CD in MeCN solution with $c = 1 \cdot 10^{-5}$ M.

[d]) Ref. [18].

[e]) Ref. [19].

[f]) Viosamine or 4-amino-4,6-dideoxy-β-D-glucopyranose.

of synthetic standards having β-D-configuration, however, have been prepared and compared with the corresponding α-D-derivatives (see *e.g. Figs. 5, 9,* and *12*): the small degree of variation can serve to estimate the amount of variation to be expected in other cases between oligosaccharide-conversion products with β-D- or β-L-configuration and synthetic standards with α-D- or α L-configuration.

**7. Structure Identification Using the CD Data Base.** – Oligosaccharide-conversion products can be classified according to the numbers of each chromophore present on the basis of UV analysis, as outlined above in *Chapt. 5* (see *Table 1*). The CD data has been divided into these different classes to allow for easy comparison of the various isomers in each class.

7.1. *Tris- and Tetrakis(4-bromobenzoates).* When UV analysis indicates the presence of 4-bromobenzoate chromophores only, MS must be used to determine the number of these chromophores (see *Chapt. 5*). Such compounds are derived from the terminal sugar units of oligosaccharides and, thus, will always be obtained in oligosaccharide-conversion mixtures. As the CD curves of these derivatives generally vary only in sign and intensity, the corresponding data have been tabulated (see *Table 2*). The difference in $\Delta\varepsilon$ values between extrema, or amplitude *(A)*, is included in *Table 2* for convenient comparison.

$B_3C$-, $BC_3$-, *and* $B_2C_2$-*Tetrachromophoric Derivatives.* The spectra for these classes are given in *Figs. 4–10* and arranged in such a way that similar spectra, *i.e.*, those having *Cotton* effects (E) with the same sign, are nearby to facilitate comparison. While these spectra correspond to linked and branched gluco-, galacto-, and mannopyranosides, they are also applicable to *N*-benzoylated compounds which are obtained from GlcNAc and GalNAc residues. In *Scheme 5*, Gal*NBBB* and Glc*NBBBC* were obtained from the cleavage of sarasinoside $C_1$. As shown in *Table 2*, the Gal*NBBB* data *(Entry 4)* are in excellent agreement with the corresponding *O*-(4-bromobenzoate) data *(Entry 3)*. Similarly, as depicted in *Fig. 5 (Spectrum 12)*, the CD curve of Glc*NBBBC* is in good agreement with that of Glc*BBBC*.

7.2. $B_2C$- *and* $BC_2$-*Trichromophoric Derivatives.* These spectra are arranged in *Figs. 11–24* in a similar manner as described above. Unlike the tetrachromophoric derivatives, however, the trichromophoric derivatives comprise a wide variety of sugars depending on the functionality of the position lacking a chromophore, *e.g.*, deoxy, *N*-acetyl, *O*-acetyl, and *O*-methyl. The calculated spectra are those of the *O*-acetyl derivatives but are applicable to cases with different nonchromophoric functionality, including deoxysugars. Many of the structures shown in *Figs. 11–24* correspond to commonly encountered sugar components (*i.e.*, fucose (Fuc), rhamnose (Rha), GlcNAc, and GalNAc), a number of which have been prepared synthetically or obtained from model studies. Calculations for derivatives lacking a chromophore at the 6-position correspond not only to 6-deoxyhexopyranosides but to pentopyranosides as well. Thus, for example, L-fucose (R=$CH_3$, *Fig. 13*) and D-arabinopyranose (R=H) derivatives are expected to have similar spectra, as are xylopyranose and quinovose ( = 6-deoxyglucose; Qui) derivatives *(Figs. 11, 15,* and *16)*. While HPLC retention time can clearly differentiate 2-deoxy from 2-acetamido derivatives, differentiation between 6-deoxyhexopyranose and the corresponding pentopyranose derivatives having chromophores in the same orientation requires either MS ($CH_3$ *vs.* H) or an additional sugar analysis.

**8. Analysis of CD Spectra.** – A majority of the tetrachromophoric components can be uniquely characterized by their CD spectra. For the more numerous trichromophoric derivatives, two or more possible structures correspond to a number of spectral types. In many cases, careful analysis of the absolute and relative intensities of constituent CE's makes it possible to differentiate between spectra having similar shapes.

8.1. $B_3C$-*Isomers* (see *Spectra 1–12, Figs. 4* and *5*). These spectra correspond to the 12 possible components obtainable, from hexopyranosides bearing a single linkage. In Gal*BBBC* and Man*BBBC (Spectra 1* and *7*, resp.), the spatial arrangement of the 3 *B* groups which make the dominant contributions to the CD's are approximately enantiomeric, accounting for the nearly opposite CD's of these two derivatives. Gal*BBBC*/

Glc*BBCB* (*Spectra 1* and *2*, resp.) and Man*BBBC*/Glc*CBBB* (*Spectra 7* and *8*, resp.) have similar CD's but can be differentiated on the basis of their intensities. For the discriminations among *Spectra 3–5* and among *Spectra 9–12*, the absolute intensities as well as the relative intensities between the extrema must be considered.

8.2. $BC_3$-*Isomers* (see *Spectra 13–24*, *Figs. 6* and *7*). These spectra correspond to the 12 possible components obtainable from hexopyranosides bearing three linkages. *Spectrum 13* can be differentiated from *14*/*15*, and similarly *19* from *20*/*21*, by the more intense couplet in *13* and *19*. Discrimination between *14* and *15*, and between *20* and *21* is less obvious and requires comparisons of relative intensities at extrema. Thus, an intensity ratio of 0.7 or higher between $\Delta\varepsilon_{287}$ and $\Delta\varepsilon_{323}$ favors *14* over *15* (ratio *ca.* 0.4). In the case of *16* and *17*, both calculated curves are of similar intensities at their $\lambda_{extr.}$; Gal*CBCC* and Gal*BCCC*, however, can be distinguished from the different shapes of the experimental curves (see *Spectra 16* and *17*).

8.3. $B_2C_2$-*Isomers* (see *Spectra 25–42*, *Figs. 8–10*). These spectra correspond to the 18 possible components obtainable from hexopyranosides bearing two linkages (branching sugars). They can be divided into several subgroups on the basis of overall shape, *i.e.*, *Spectra 25*/*26*, *27*/*28*, *29*/*30*, *31–36*, and *37–39*; *40–42* have shapes which are different from the others. Spectra within each subgroup can be characterized by differing intensities of their CE's, *e.g.*, *31*/*32*, *36*/*33–35*, and *39*/*37* and *38*. Discrimination within each subgroup, *i.e.*, *25*/*26*, *27*/*28*, *29*/*30*, *33*/*34*/*35*, and *37*/*38* requires determination of experimental $\Delta\varepsilon$ values within the range 220–360 nm and comparison of the relative intensities of the various *Cotton* effects.

A comparison between calculated CD's in *Spectra 29* and *30* reveals clear differences below 240 and above 300 nm. It may, however, be difficult to distinguish between Man*CBBC* and Man*BBCC*, because, although the agreement between the calculated and observed values of Man*CBBC* is fair, the CD of an authentic Man*BBCC* sample has not yet been recorded (*Spectra 29* and *30*). In *Spectrum 36*, the agreement between calculated and experimental curves is also poor; in such cases the experimental curve should be used for comparison.

8.4. $B_2C$-*Isomers* (see *Spectra 43–84*, *Figs. 11–17*). These spectra correspond to 42 possible components, also representative for *N*-acetylated aminodeoxyhexopyranose, deoxyhexopyranose, or pentopyranose sugars, all having a single linkage. Depending on the shape of the entire CD curve and relative intensities of the constituent CE's, these 42 spectra have been further divided into three groups to facilitate comparison for structure elucidation.

8.4.1. *Spectra 43–54*. CD curves in this subgroup are characterized by a strong positive CE around 250 nm and a broad weak negative CE in the region 270–340 nm; in *Spectra 43–45*, *51*, and *53*, a second very weak CE is present at 230 nm. *Spectra 43–45* can be readily differentiated from *46* to *53* on the basis of their intense 250-nm CE ($\Delta\varepsilon > 45$). While differentiation between *43*, *44*, and *45* cannot be certain because the shapes and intensities of CD are similar, they are derived from different sugars, the identities of which can be readily determined using conventional sugar analyses; the same is true for cases *46–48* when the experimentally measured $\Delta\varepsilon$'s at 250 nm fall within the range 25–35.

While the differentiation between GlcA*CBCB* and ManA*CBCB* is not feasible (*Spectra 49* and *50*), these two can be distinguished from *51* to *53* on the following grounds. Regardless of the similar positive CE around 250 nm for all 5 cases *49–53*, only *51* and *52*

display broad negative bands above 260 nm with distinctive shape with $\lambda_{extr.}$ around 311 nm, whereas only *53* exhibits an extremely weak negative band ($\Delta\varepsilon = -2$) above 260 nm.

8.4.2. *Spectra 55–60.* These 6 spectra possess similar shapes with a positive first CE at the shortest wavelength ($\lambda_1$) and two additional negative CE's at longer wavelengths ($\lambda_2$, $\lambda_3$). The pairs *55/56*, *57/58*, and *59/60* can be clearly distinguished from the differences in respective $\Delta\varepsilon$ values and also from the intensity ratios $\Delta\varepsilon(\lambda_1)/\Delta\varepsilon(\lambda_2)$ and $\Delta\varepsilon(\lambda_2)/\Delta\varepsilon(\lambda_3)$. As each pair consists of, *e.g.*, an L-fucose (R = Me) and a D-rhamnose (R = Me) derivative, further differentiation here would simply require knowledge of which of these two sugars was present.

8.4.3. *Spectra 61–72.* The CD curves of *Spectra 61*, *62*, and *72* exhibit characteristic features that allow them to be distinguished from the others, but precise measurements down to 220 nm is necessary. The similarity between *63* and *64* again results from the nearly identical spatial arrangement of chromophores in D-fucose (R = Me) and L-rhamnose (R = Me) derivatives, respectively. This also applies to *67/68* and *70/71*. Making a positive identification in these cases will again simply require knowledge of which of the two possible sugars is expected. The different intensity ratios of CE's at *ca.* 250 nm and *ca.* 300 nm clearly distinguishes *67/68/70/71* from *69*.

8.4.4. *Spectra 73–84.* The 12 cases belonging to this subgroup are characterized by 3 distinct bands: positive CE at *ca.* 235 nm ($\lambda_1$), negative CE at *ca.* 250 nm ($\lambda_2$), and a broad positive band centered around 310 nm ($\lambda_3$). A detailed examination reveals that in *73–76* and *79*, the intensity ratio $\Delta\varepsilon(\lambda_2)/\Delta\varepsilon(\lambda_3)$ is *ca.* 6 or higher, while in cases *77/78/80–84* this ratio is 1–3. Although the pairs *73/74* and *75/76* have similar $\Delta\varepsilon(\lambda_2)/\Delta\varepsilon(\lambda_3)$ ratios and $\Delta\varepsilon(\lambda_2)$ values, the four cases can be differentiated because ManAc*BBC* and GlcAc*BBC* (*Spectra 73* and *75*, resp.) have stronger positive $\Delta\varepsilon(\lambda_1)$ values of 10–15. While it may not be possible to distinguish GalAc*BCB* from Glc*BC*Ac*B* (*Spectra 78* and *81*, resp.), the former would likely derive from a 4-linked GalNAc, while the latter corresponds to a 3-linked glucose residue which is either deoxygenated or substituted at position 4; MS can readily clarify any ambiguities. Analogously, the very similar *Spectra 83* and *84* correspond to widely different sugar types.

8.5. $BC_2$-*Isomers* (see *Spectra 85–126*, *Figs. 18–24*). These spectra correspond to 42 possible components, also representative for *N*-acetylated aminodeoxyhexopyranose, deoxyhexopyranose, or pentopyranose sugars, all having two linkages (branched). The spectra can be divided into seven subgroups.

8.5.1. *Spectra 85–90.* These 6 CD spectra possess a very strong negative couplet; the negative wing with $\lambda_{extr.}$ at *ca.* 320 nm ($\lambda_2$) is of higher intensity than the positive wing at *ca.* 285 nm ($\lambda_1$). It is possible to discriminate *Spectra 85–87* from *88–90* on the basis of the intensities at $\lambda_1$ and $\lambda_2$. The distinction among *85–87* is uncertain except for the weak negative CE around 235 nm in *86*, but they should be readily differentiated by MS. In *88–90*, differences are seen in the short-wavelength region of calculated curves; however, lack of experimental curves for *88* and *90* leads to uncertainty. Again MS can clarify the differences.

8.5.2. *Spectra 91–96.* The *Spectra 91* and *96* of GalAc*CBC* and Gal*C*Ac*BC*, respectively, are distinctly different from *92* to *95*, the latter group being characterized by a series of weak negative, positive, and negative CE's in the range 220–360 nm. Although pair *92/93* can be distinguished from pair *94/95*, further differentiation within each pair is not possible without additional structural information.

8.5.3. *Spectra 97–102. Spectra 97–100* corresponding to two L-fucose and two D-rhamnose derivatives are found to have very similar CD patterns; only *Spectrum 100* can be differentiated by its smaller $\Delta\varepsilon$ value at 315 nm and the intensity ratio of $\Delta\varepsilon_{246}/\Delta\varepsilon_{314}$. While most cases of similar spectra involve different sugars, the similarity between *97* and *99*, both derived from L-fucose, makes it impossible to distinguish between 3,4- and 2,4-branched L-fucose components by this method. Differentiation between *101* and *102* which are both derived from mannose also appears to be difficult.

8.5.4. *Spectra 103–111.* In these 9 cases, *103–107* and *108–111* show, respectively, intense and moderately intense positive couplets with CE's at *ca.* 287 nm ($\lambda_1$) and 323 nm ($\lambda_2$). Further identification, however, requires careful estimation of not only the $\Delta\varepsilon$ of the 2 wings, but also the intensity ratio $\Delta\varepsilon(\lambda_1)/\Delta\varepsilon(\lambda_2)$. From such measurements, *104* can reliably be differentiated from *103* and *105–107*, and similarly *111* from *109* and *110*.

8.5.5. *Spectra 112–116.* These 5 cases are clearly differentiated by the relative intensities of their three major CE's. Notable differences are also seen in the 220–250-nm range.

8.5.6. *Spectra 117–120.* Despite the very poor agreement between calculated and experimental curves in Glc*BC*Ac*C* (*Spectrum 120)*, this spectrum should be readily distinguishable from *117* to *119* where no further differentiation is possible. Similarity between *118* and *119*, both derived from D-fucose, makes it impossible to distinguish between 3,4- and 2,4-branched D-fucose components by this method as discussed above for the enantiomeric L-fucose components (*Spectra 97* and *99*).

8.5.7. *Spectra 121–126. Spectra 121–123* can be readily identified from the distinctive shapes of the CD curves and different $\Delta\varepsilon$ values around 245 and 300 nm. In *Spectra 124–126*, similarities in the shape of CD curves and the close values of the strongest positive CE around 285 nm make differentiation strongly dependent upon the accuracy of measured $\Delta\varepsilon$ values and relative intensity ratios of the three CE's.

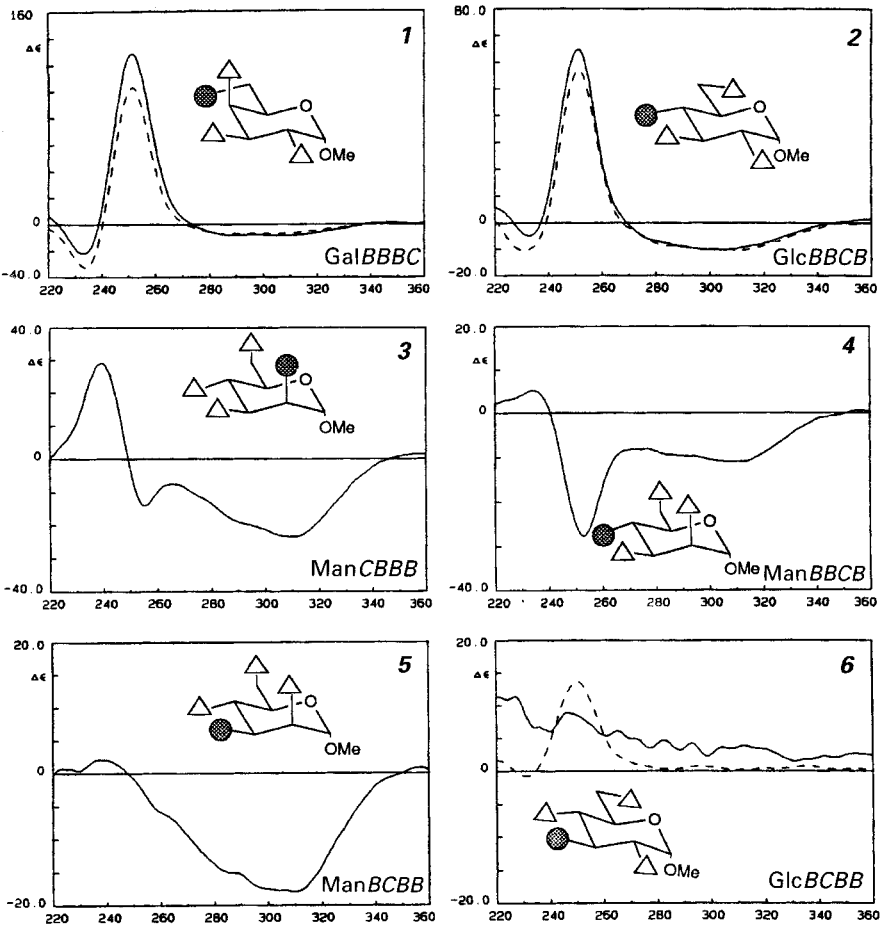


Fig. 4. *CD Spectra of* $B_3C$*-substituted derivatives.*

*1*) Calc.: 233 (−22), 252 (+128); found for α-D-anomer: 234 (−32.3), 252 (+102.0), 285 (−7.4).

*2*) Calc.: 233 (−5), 252 (+65); found for α-D-anomer: 230 (−10.5), 252 (+56.8), 311 (−10.4).

*3*) Calc.: 239 (+29), 255 (−14), 310 (−23).

*4*) Calc.: 234 (+5), 253 (−28), 285 (sh, −10), 314 (−11).

*5*) Calc.: 240 (+2), 285 (sh, −15), 310 (−18).

*6*) Calc.: 228 (+11), 247 (+9), 305 (+4); found for α-D-anomer: 232 (−0.8), 251 (+13.5), 296 (+0.7).

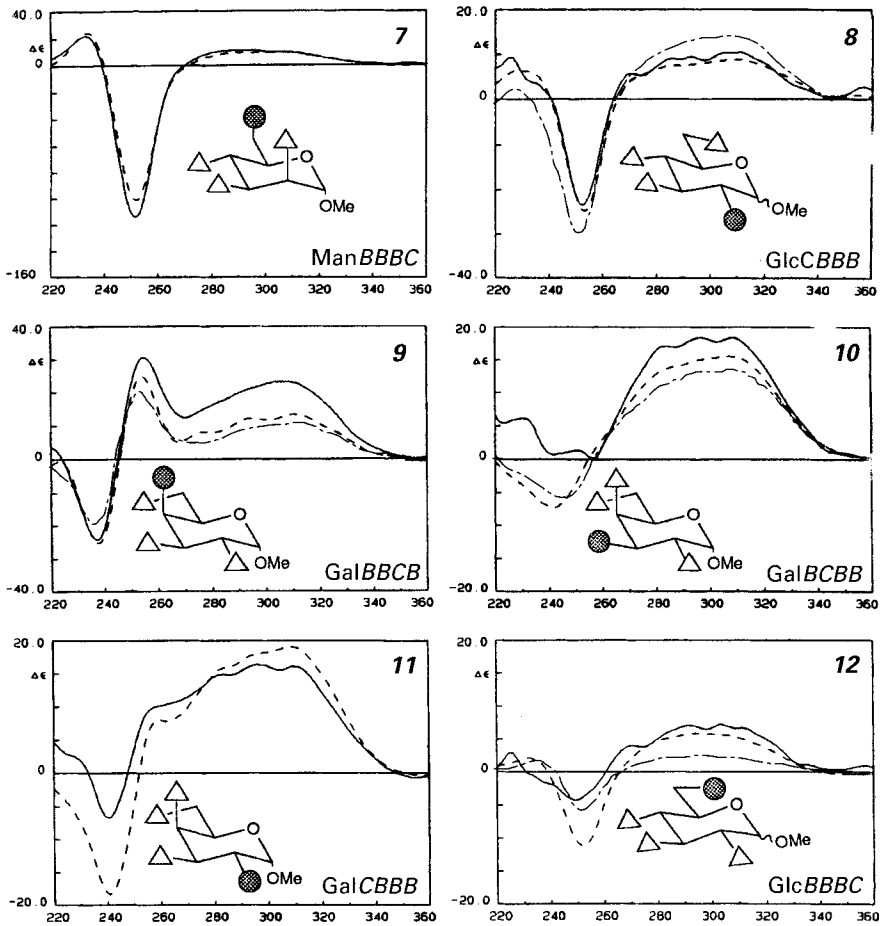


Fig. 5. *CD Spectra of* $B_3C$-*substituted derivatives* (continued).

*7*) Calc.: 233 (+22), 252 (−113), 291 (+11); found for α-D-*anomer*: 234 (+24.7), 252 (−100.0), 287 (+8.9), 309 (+9.4).

*8*) Calc.: 226 (+9), 252 (−23), 270 (sh, +6), 284 (sh, +9), 307 (+10); found for α-D-anomer (– – –): 228 (+6.3), 253 (−24.5), 286 (sh, +7.5), 310 (+8.7); found for β-D-anomer (– · – · –): 228 (+2.3), 253 (−29.5), 285 (sh, +11.4), 307 (14.2).

*9*) Calc.: 237 (−24), 254 (+31), 305 (+23); found for α-D-anomer (– – –): 238 (−25.2), 254 (+24.7), 284 (sh, +8.3), 295 (sh, +12), 311 (+13.2); found for β-D-anomer (– · – · –): 237 (−19.1), 254 (+20.1), 311 (+10.9).

*10*) Calc.: 230 (+6), 284 (+17), 296 (+18), 309 (+18); found for α-D-anomer (– – –): 241 (−7.3), 287 (sh, +14), 306 (+15.4); found for β-D-anomer (– · – · –): 246 (−5.7), 297 (+13.3), 309 (+13.6).

*11*) Calc.: 241 (−7), 258 (sh, +10), 282 (sh, +15), 296 (sh, +16), 310 (+16); found for α-D-anomer: 241 (−18.2), 259 (sh, +8.1), 285 (sh, +16), 297 (sh, +18), 309 (+19).

*12*) Calc.: 225 (+3), 250 (−4), 270 (sh, +4), 292 (sh, +7), 304 (+8); found for α-D-anomer (– – –): 233 (+2.1), 253 (−11), 296 (+5.8); found for β-D-GlcN*BBBC* (– · – · –): 236 (+1.8), 253 (−5.7), 305 (+2.4).

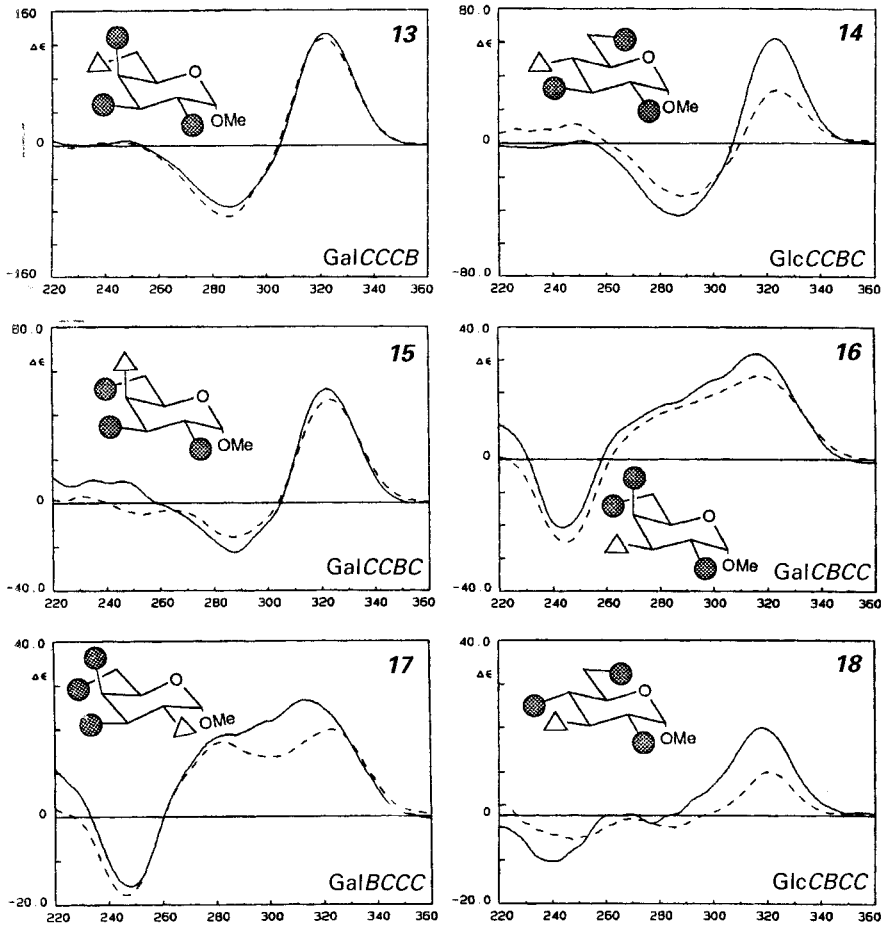


Fig. 6. *CD Spectra of* $BC_3$*-substituted derivatives.*

*13*) Calc.: 286 (−74), 322 (+132); found for α-D-anomer: 285 (−85.6), 321 (+125).
*14*) Calc.: 287 (−43), 323 (+62); found for α-D-anomer: 248 (+11.3), 289 (−31.1), 323 (+31.4).
*15*) Calc.: 288 (−23), 322 (+52); found for α-D-anomer: 287 (−15.5), 323 (+46.7).
*16*) Calc.: 244 (−21), 284 (sh, +17), 316 (+32); found for α-D-anomer: 245 (+25.1), 284 (sh, +14.7), 317 (+24.9).
*17*) Calc.: 249 (−16), 285 (sh, +19), 313 (+27); found for α-D-anomer: 247 (−17.7), 283 (+16.9), 323 (+19.7).
*18*) Calc.: 241 (−10), 318 (+20); found for α-D-anomer: 248 (−5.5), 285 (−2.7), 320 (+9.9).

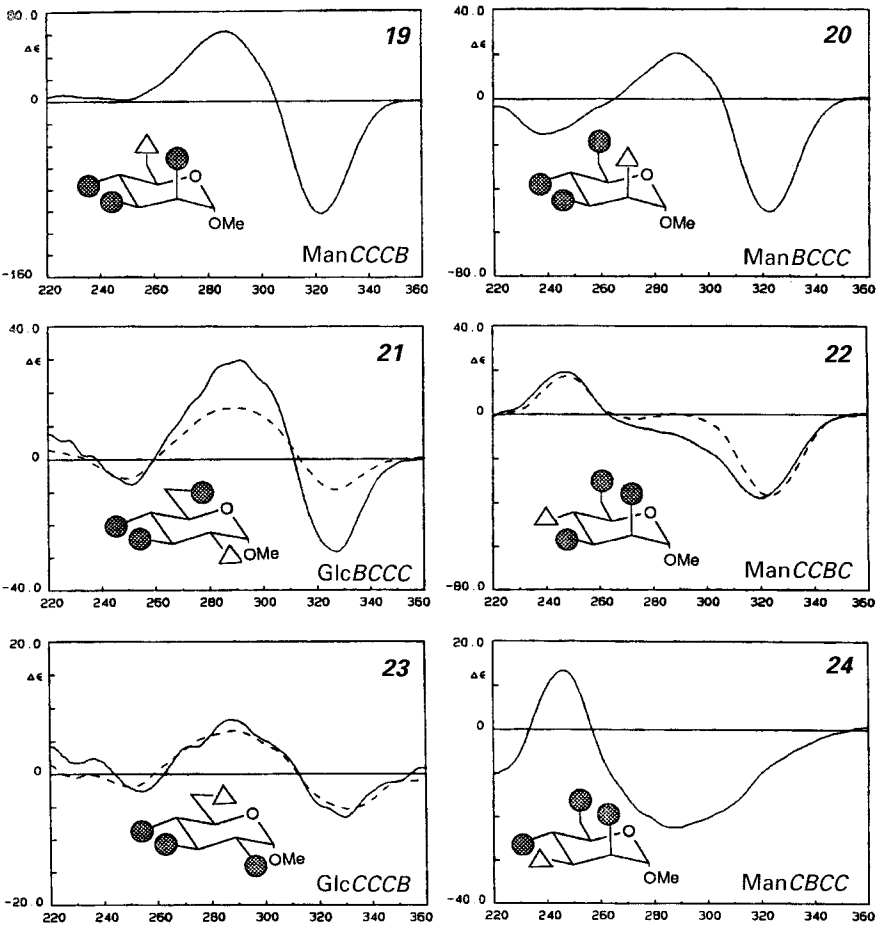


Fig. 7. *CD Spectra of* $BC_3$*-substituted derivatives* (continued).

*19*) Calc.: 286 (+63), 322 (−101).

*20*) Calc.: 238 (−15), 288 (+21), 322 (−51).

*21*) Calc.: 251 (−8), 284 (sh, +28), 292 (+30), 327 (−28); found for α-D-anomer: 249 (−5.7), 290 (+15.2), 327 (−9.2).

*22*) Calc.: 247 (+19), 319 (−38); found for α-D-anomer: 247 (+17.2), 273 (−2.1), 323 (−36.7).

*23*) Calc.: 237 (+2), 254 (−3), 287 (+8), 329 (−7); found for α-D-anomer: 250 (−2), 290 (+6.6), 331 (−5.3).

*24*) Calc.: 246 (+13), 288 (−22).

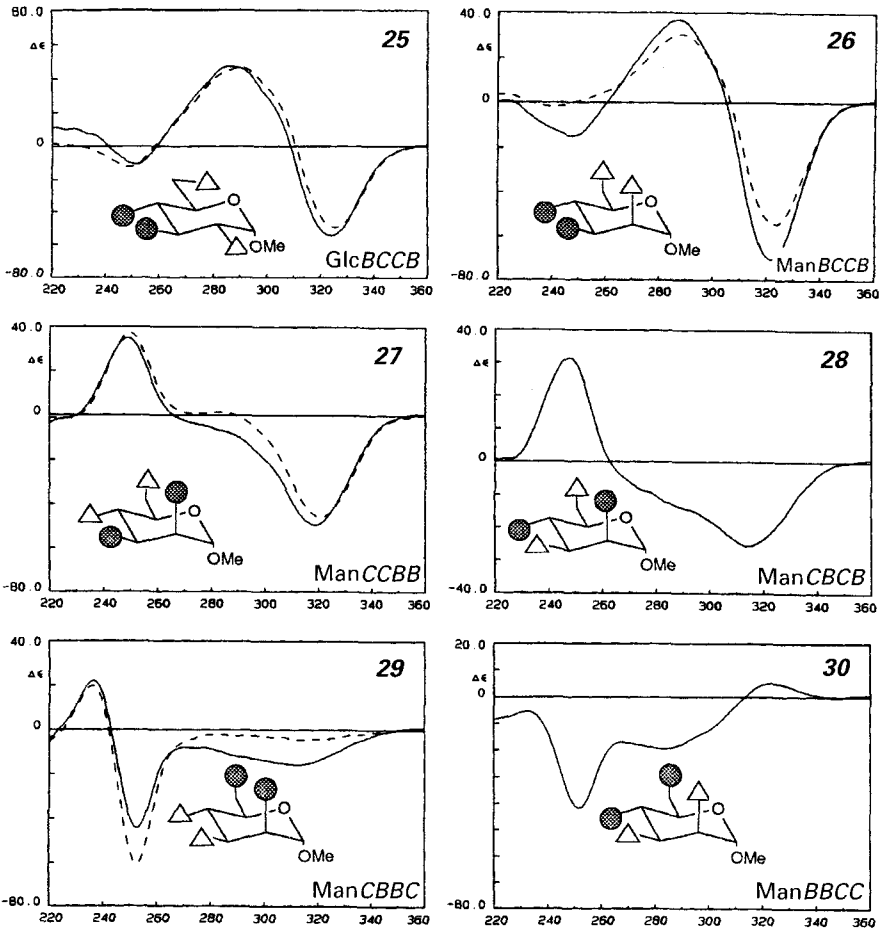


Fig. 8. *CD Spectra of* $B_2C_2$*-substituted derivatives.*

*25*) Calc.: 251 (−11), 286 (+47), 323 (−54); found for α-D-anomer: 249 (−12.1), 290 (+46.4), 325 (−49.3).

*26*) Calc.: 248 (−15), 287 (+37), 322 (−71); found for α-D-anomer: 287 (+30.3), 323 (−54.5).

*27*) Calc.: 249 (+35), 319 (−49); found for α-D-anomer: 249 (+37.3), 321 (−45.7).

*28*) Calc.: 247 (+31), 314 (−26).

*29*) Calc.: 236 (+22), 253 (−44), 313 (−16); found for α-D-anomer: 236 (+19.6), 253 (−60.6); 313 (−4.4).

*30*) Calc.: 252 (−42), 284 (−19), 323 (+5).

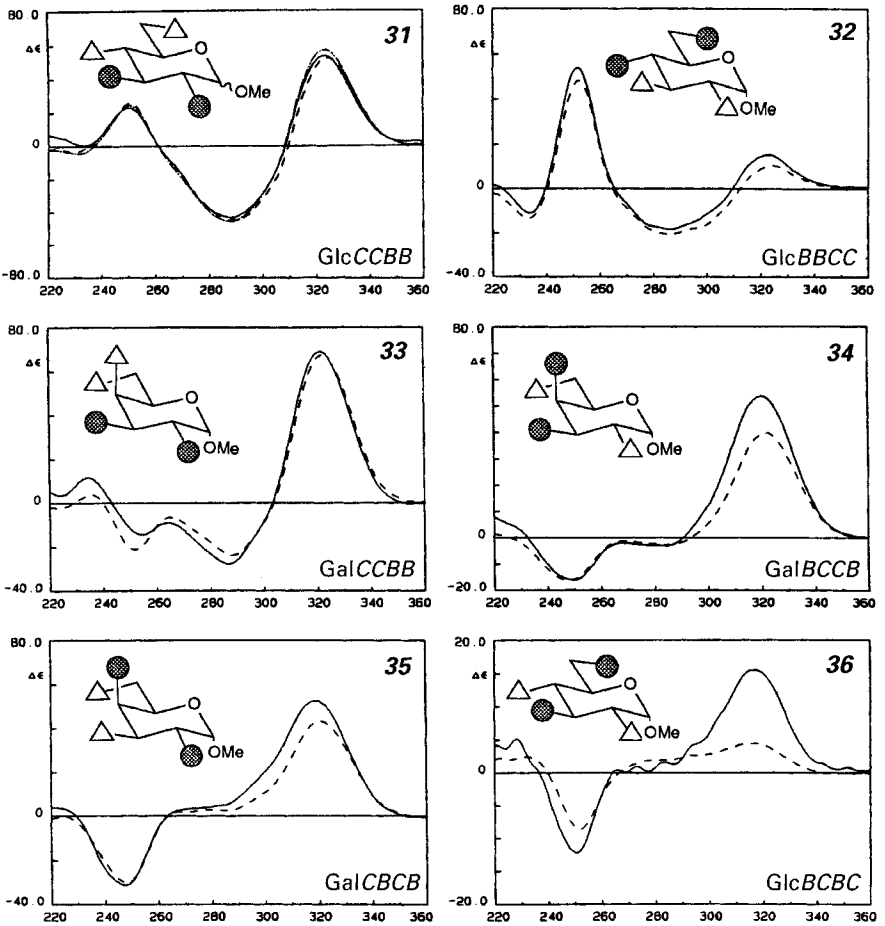


Fig. 9. *CD Spectra of* $B_2C_2$*-substituted derivatives* (continued).

*31*) Calc.: 250 (+23), 287 (−43), 323 (+54); found for α-D-anomer (– – –): 251 (+25.9), 289 (−44.6), 325 (+52.1); found for β-D-anomer: (– · – · –): 251 (+24.5), 287 (−45.4), 323 (+57).

*32*) Calc.: 234 (−11), 252 (+54), 286 (−18), 323 (+15); found for α-D-anomer: 233 (−13.3), 252 (+48.4), 286 (−20.5), 299 (sh, −16.6), 325 (+10.4).

*33*) Calc.: 235 (+12), 255 (−14), 287 (−28), 321 (+69); found for α-D-anomer: 251 (−21.2), 288 (−23.7), 322 (+67.3).

*34*) Calc.: 250 (−16), 320 (+54); found for α-D-anomer: 248 (−16.2), 284 (−2.7), 321 (+39.7).

*35*) Calc.: 247 (−31), 319 (+53); found for α-D-anomer: 248 (−30), 321 (+43.2).

*36*) Calc.: 229 (+5), 250 (−12), 295 (sh, +4), 317 (+16); found for α-D-anomer: 233 (+2.4), 252 (−8.5), 293 (+2.6), 317 (+4.5).

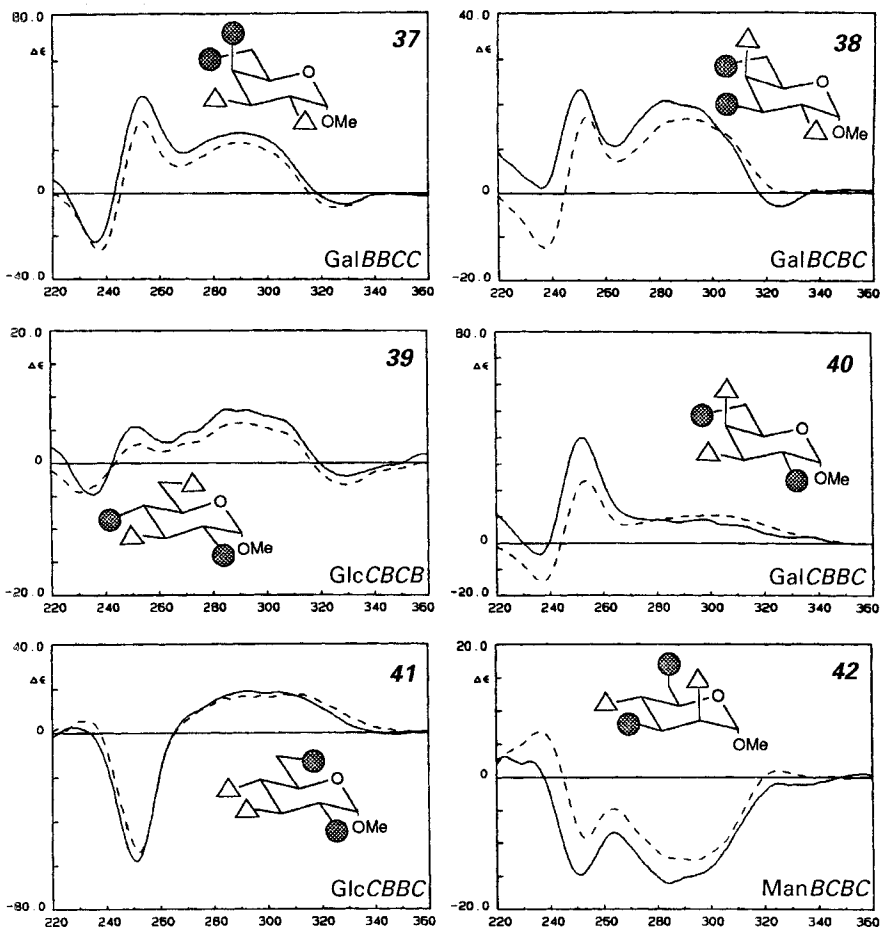


Fig. 10. *CD Spectra of* $B_2C_2$*-substituted derivatives* (continued).

*37*) Calc.: 236 (−23), 253 (+44), 290 (+28), 329 (−5); found for α-D-anomer: 238 (−26.7), 254 (+33), 290 (+23.2), 326 (−6.4).

*38*) Calc.: 251 (+23), 283 (+21), 292 (sh, +19), 324 (−3); found for α-D-anomer: 237 (−12.5), 253 (+17.1), 290 (+16.5).

*39*) Calc.: 235 (−5), 251 (+5), 285 (+8), 293 (sh, +8), 330 (−2); found for α-D-anomer: 231 (−4.4), 253 (+2.9), 269 (sh, +2.9), 292 (+6.1), 306 (sh, +4.6), 329 (−3.3).

*40*) Calc.: 236 (−4), 252 (+40), 296 (+9); found for α-D-anomer: 237 (−14.5), 253 (+23.6), 302 (+10.4).

*41*) Calc.: 228 (+3), 251 (−58), 293 (+19); found for α-D-anomer: 232 (+5.4), 252 (−53.7), 284 (sh, +15.7), 299 (sh, +16.8), 306 (+17.3).

*42*) Calc.: 223 (+3), 233 (sh, +2), 251 (−15), 284 (−16); found for α-D-anomer: 236 (+6.9), 253 (−9.3), 283 (sh, −12.2), 294 (−12.5), 325 (+0.9).

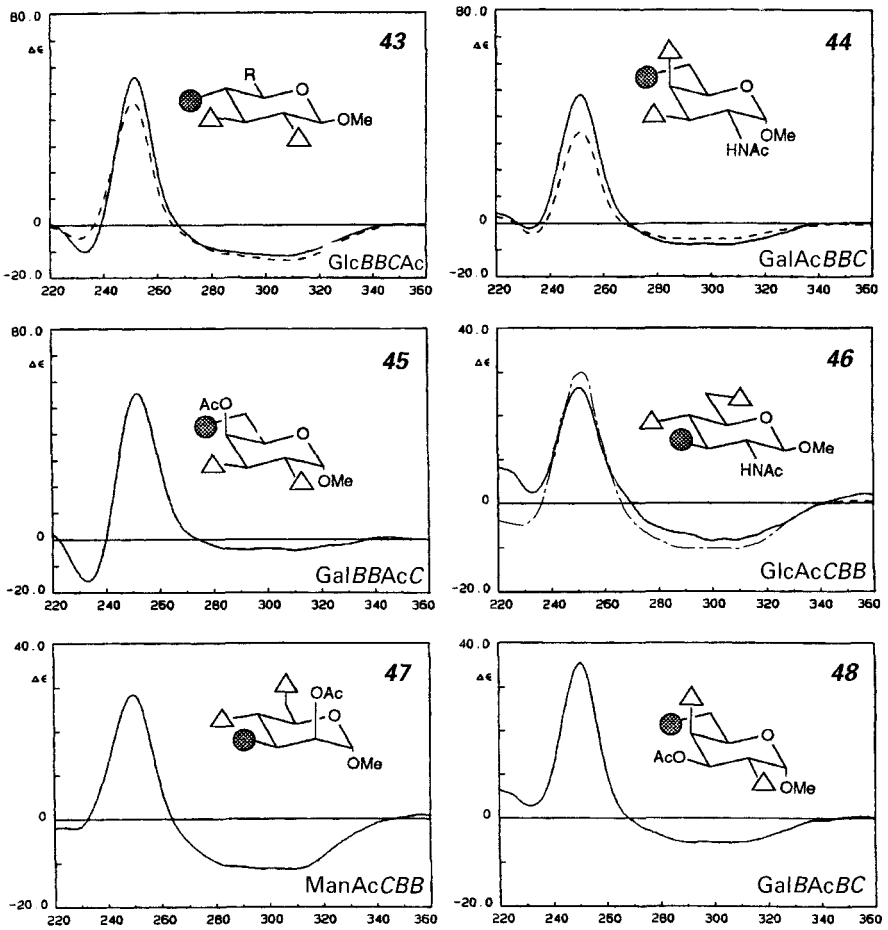


Fig. 11. *CD Spectra of* $B_2$C-*substituted derivatives* (continued).

*43*) D-Xyl*pBBC* (R = H) or D-Qui*BBC* (R = Me); calc.: 233 (−10), 252 (+56), 306 (−12); found for β-D-Xyl*BBC*: 231 (−5.0), 251 (+46.4), 310 (−13.2).

*44*) Calc.: 220 (+4), 233 (−2), 251 (+48), 304 (−8); found for α-D-GalNAc*BBC*: 233 (−4), 251 (+34.3), 294 (−6).

*45*) Calc.: 233 (−16), 252 (+56), 307 (−4).

*46*) Calc.: 221 (+8), 250 (+26), 299 (−9); found for β-D-GlcNAc*CBB*: 227 (−4.9), 251 (+30), 304 (−10.3).

*47*) Calc.: 249 (+28), 284 (−11), 311 (−11).

*48*) Calc.: 251 (+35), 291 (−6), 303 (−5).

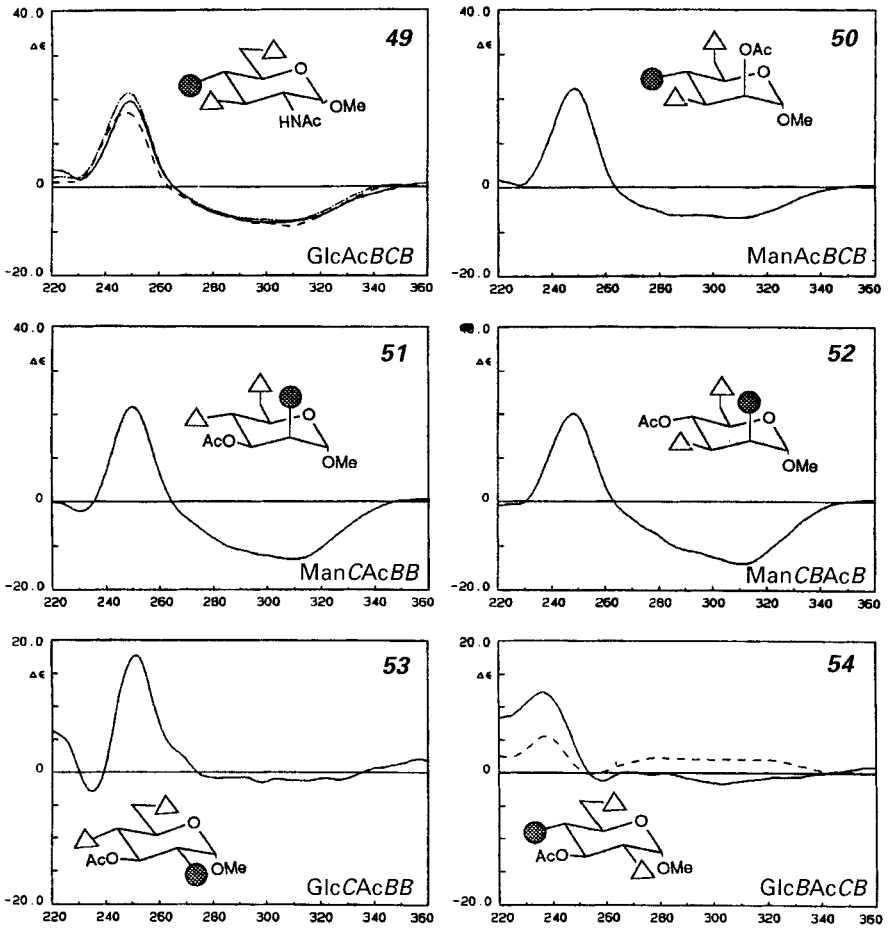


Fig. 12. *CD Spectra of* $B_2C$-*substituted derivatives* (continued).

*49*) Calc.: 249 (+20), 304 (−8); found for α-D-GlcNAc*BCB* (– – –): 247 (+17), 296 (sh, −8.2), 309 (−8.9); found for β-D-GlcNAc*BCB* (– · – · –): 248 (+21.5), 308 (−7.6).

*50*) Calc.: 248 (+22), 283 (sh, −6), 311 (−7).

*51*) Calc.: 231 (−2), 250 (+22), 311 (−13).

*52*) Calc.: 248 (+20), 293 (sh, −11), 311 (−14).

*53*) Calc.: 218 (+7), 234 (−3), 251 (+18), 298 (−2).

*54*) Calc.: 237 (+12), 259 (−1), 302 (−2); found for α-D-anomer: 238 (+5.5), 280 (+2.3), 320 (+2).

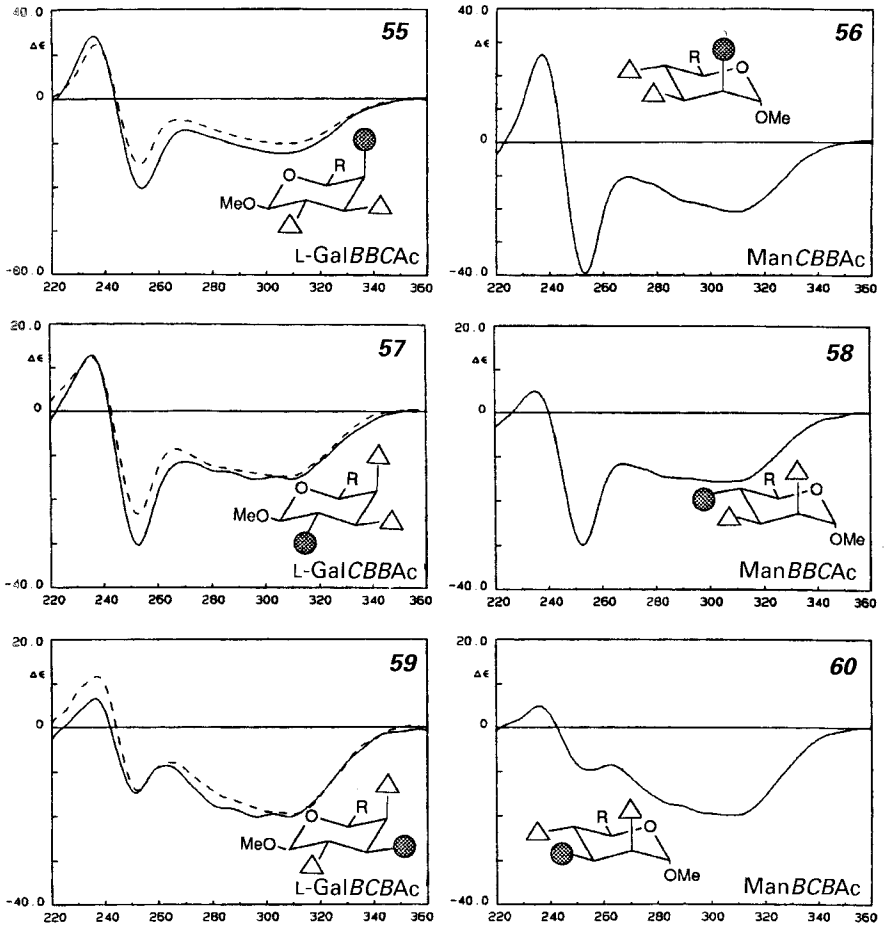


Fig. 13. *CD Spectra of* $B_2$C-*substituted derivatives* (continued).

*55*) L-Fuc*BBC* (R = Me) or D-Ara*pBBC* (R = H); calc.: 236 (+28), 254 (−40), 306 (−24); found for β-L-Fuc*BBC*: 237 (+24.5), 253 (−29.4), 311 (−19.6).

*56*) D-Rha*CBB* (R = Me); calc.: 237 (+26), 253 (−40), 310 (−21).

*57*) L-Fuc*CBB* (R = Me) or D-Ara*pCBB* (R = H); calc.: 236 (+13), 253 (−30), 283 (sh, −14), 310 (−15); found for β-L-Fuc*CBB*: 236 (+12.3), 253 (−23.4), 283 (sh, −12.8), 310 (−14.7).

*58*) D-Rha*BBC* (R = Me); calc.: 235 (+5), 252 (−30), 283 (sh, −14), 311 (−15).

*59*) L-Fuc*BCB* (R = Me) or D-Ara*pBCB* (R = H); calc.: 236 (+7), 251 (−15), 284 (sh, −18), 297 (−20), 308 (−20); found for β-L-Fuc*BCB*: 237 (+11.6), 252 (−14.2), 300 (−18.9), 311 (−19.4).

*60*) D-Rha*BCB* (R = Me); calc.: 236 (+5), 254 (−10), 286 (sh, −17), 303 (−20), 311 (−20).

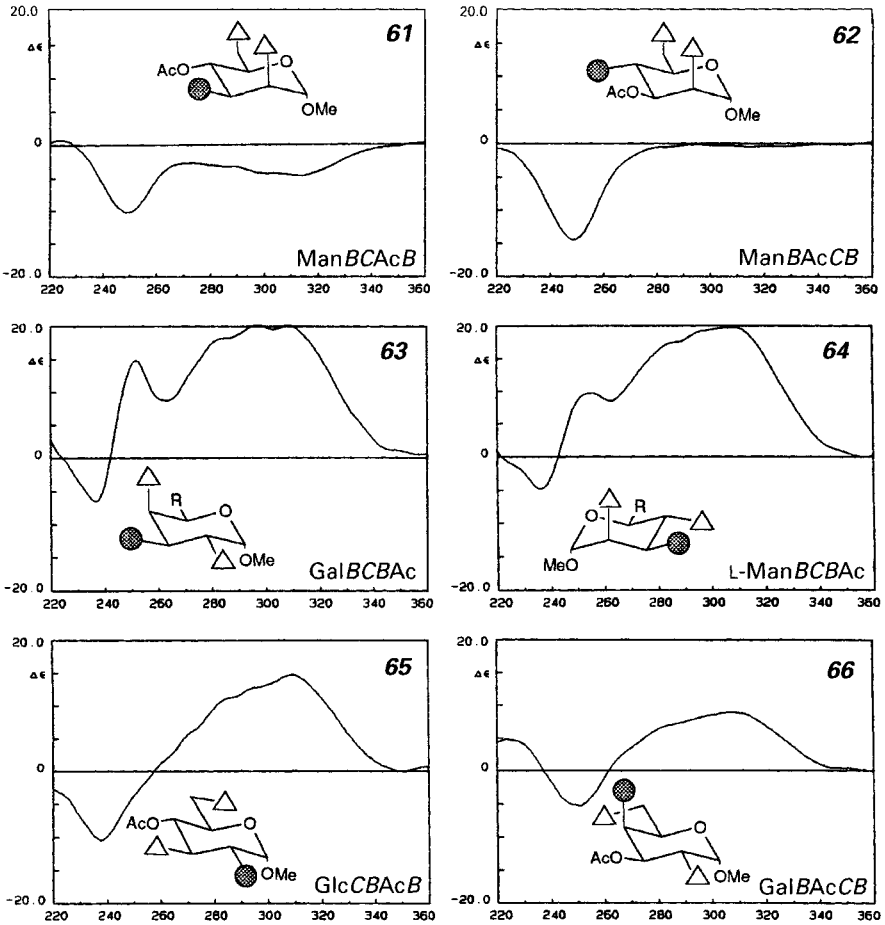


Fig. 14. *CD Spectra of* $B_2C$*-substituted derivatives* (continued).

*61*) Calc.: 249 (−10), 284 (sh, −3), 299 (sh, −4), 314 (−5).

*62*) Calc.: 248 (−14), 315 (−1).

*63*) D-Fuc*BCB* (R = Me) or L-Ara*pBCB* (R = H); calc.: 236 (−7), 251 (+15), 284 (sh, +18), 297 (+20), 308 (+20); found: see *Spectrum 59*.

*64*) L-Rha*BCB* (R = Me); calc.: 236 (−5), 254 (+10), 286 (sh, +17), 303 (+20), 311 (+20).

*65*) Calc.: 238 (−10), 309 (+15).

*66*) Calc.: 225 (+5), 250 (−5), 307 (+9).

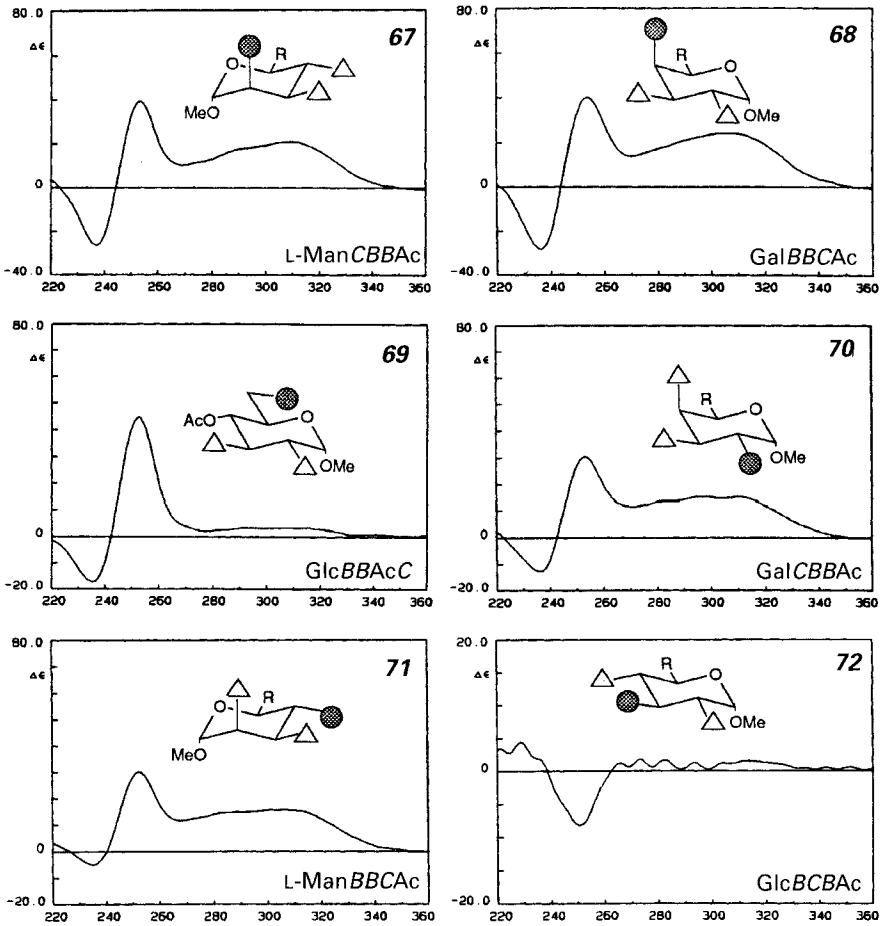


Fig. 15. *CD Spectra of* $B_2$C-*substituted derivatives* (continued).

*67*) L-Rha*CBB* (R = Me); calc.: 237 (−26), 253 (+40), 310 (+21).

*68*) D-Fuc*BBC* (R = Me) or L-Ara*pBBC* (R = H); calc.: 236 (−28), 254 (+40), 306 (+24); found: see *Spectrum 55*.

*69*) Calc.: 236 (−17), 252 (+45), 305 (+3).

*70*) D-Fuc*CBB* (R = Me) or L-Ara*pCBB* (R = H); calc.: 236 (−13), 253 (+30), 283 (sh, +14), 310 (+15); found: see *Spectrum 57*.

*71*) L-Rha*BBC* (R = Me); calc.: 235 (−5), 252 (+30), 283 (sh, +14), 311 (+15).

*72*) D-Xyl*pBCB* (R = H) or D-Qui*BCB* (R = Me); calc.: 229 (+4), 251 (−8), 314 (+2).

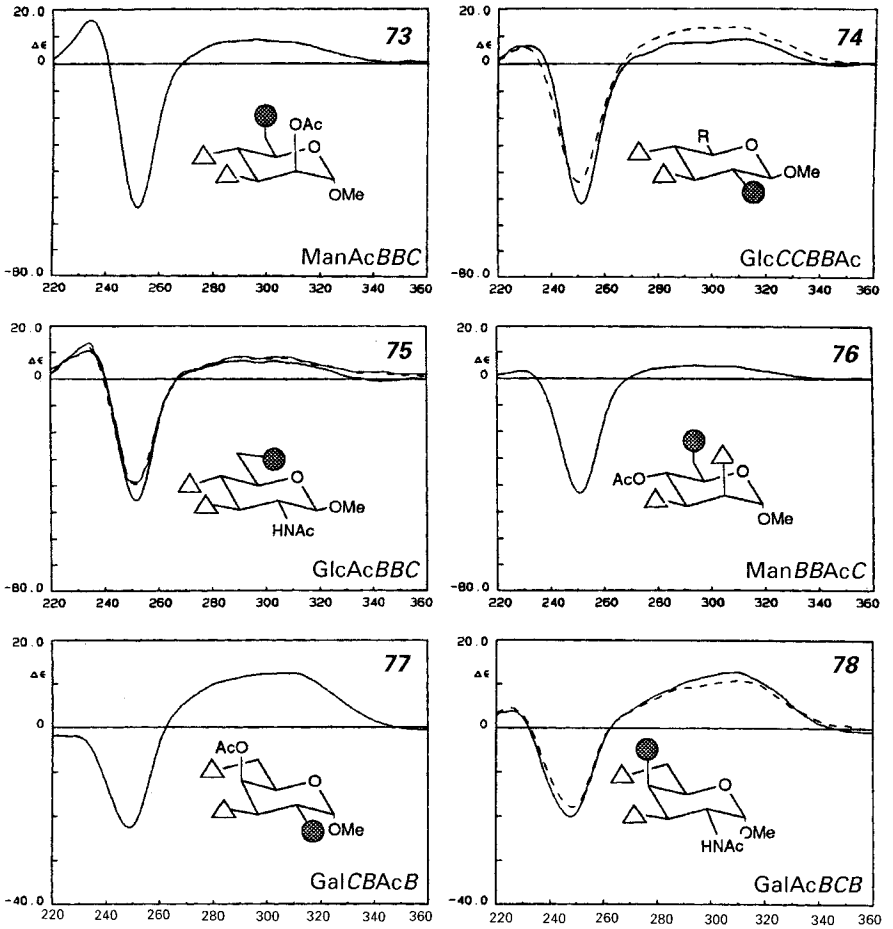


Fig. 16. *CD Spectra of* $B_2$C-*substituted derivatives* (continued).

*73*) Calc.: 234 (+16), 252 (−54), 282 (sh, +8), 296 (+9), 311 (sh, +8).

*74*) D-Xyl*pCBB* (R = H) or D-Qui*CBB* (R = Me); calc.: 230 (+6), 251 (−52), 286 (sh, +8), 294 (sh, +8), 311 (+9); found for *β*-D-Xyl*CBB*: 229 (+5.9), 251 (−43.6), 295 (sh, +12.9), 311 (+13.2).

*75*) Calc.: 234 (+11), 252 (−46), 292 (+7), 303 (+7); found for *β*-D-GlcNAc*BBC*: 233 (+12.3), 251 (−39.5), 289 (+8.5).

*76*) Calc.: 231 (+3), 251 (−43), 282 (sh, +4), 295 (+5), 309 (sh, +4).

*77*) Calc.: 249 (−23), 283 (sh, +11), 308 (+12).

*78*) Calc.: 225 (+4), 248 (−20), 309 (+13); found for *α*-D-GalNAc*BCB*: 226 (+4.6), 249 (−17.8), 293 (sh, +9.2), 311 (+10.8).

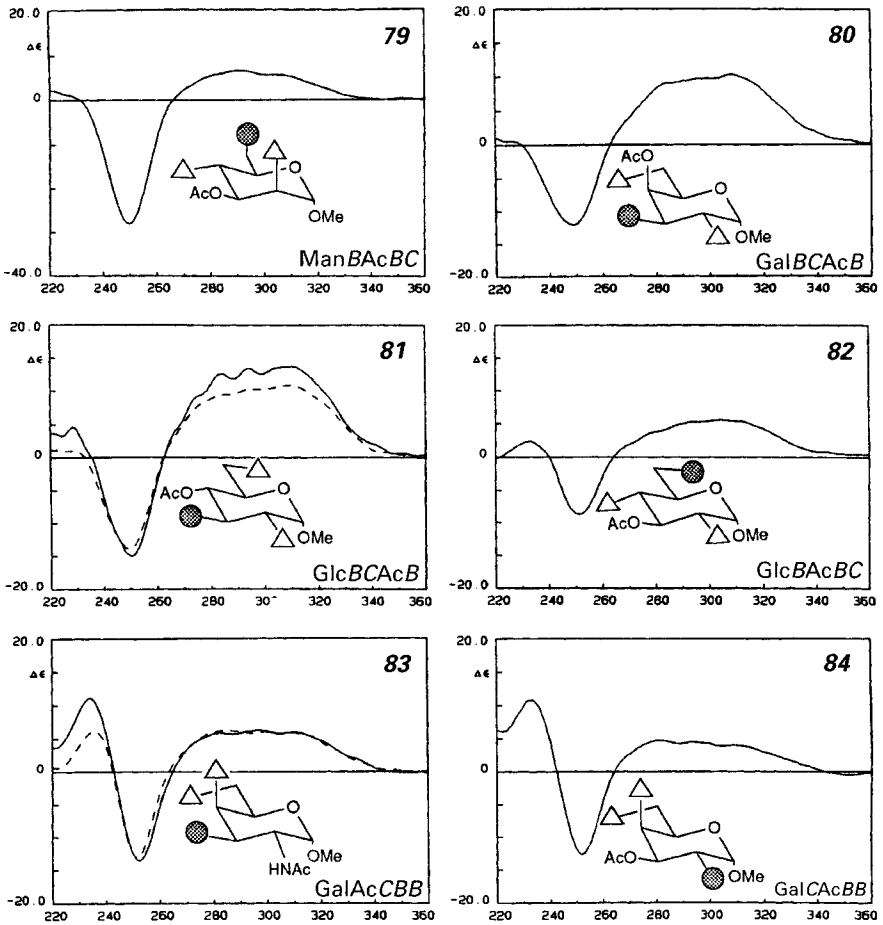


Fig. 17. *CD Spectra of* $B_2C$*-substituted derivatives* (continued).

*79*) Calc.: 250 (−28), 291 (+7), 311 (sh, +5).

*80*) Calc.: 248 (−12), 284 (sh, +9), 308 (+10).

*81*) Calc.: 229 (+5), 250 (−15), 284 (sh, +13), 310 (+14); found for α-D-anomer: 250 (−13.8), 284 (sh, +9.4), 294 (sh, +10.3), 309 (+10.8).

*82*) Calc.: 233 (+2), 251 (−9), 280 (sh, +4), 303 (+6), 311 (sh, +5).

*83*) Calc.: 234 (+11), 252 (−13), 283 (+6), 297 (+6), 311 (+6); found for α-D-GalNAc*CBB*: 236 (+6.1), 252 (−13), 285 (+6.2), 309 (+5.8).

*84*) Calc.: 233 (+11), 252 (−13), 282 (+5), 294 (sh, +4), 309 (sh, +4).

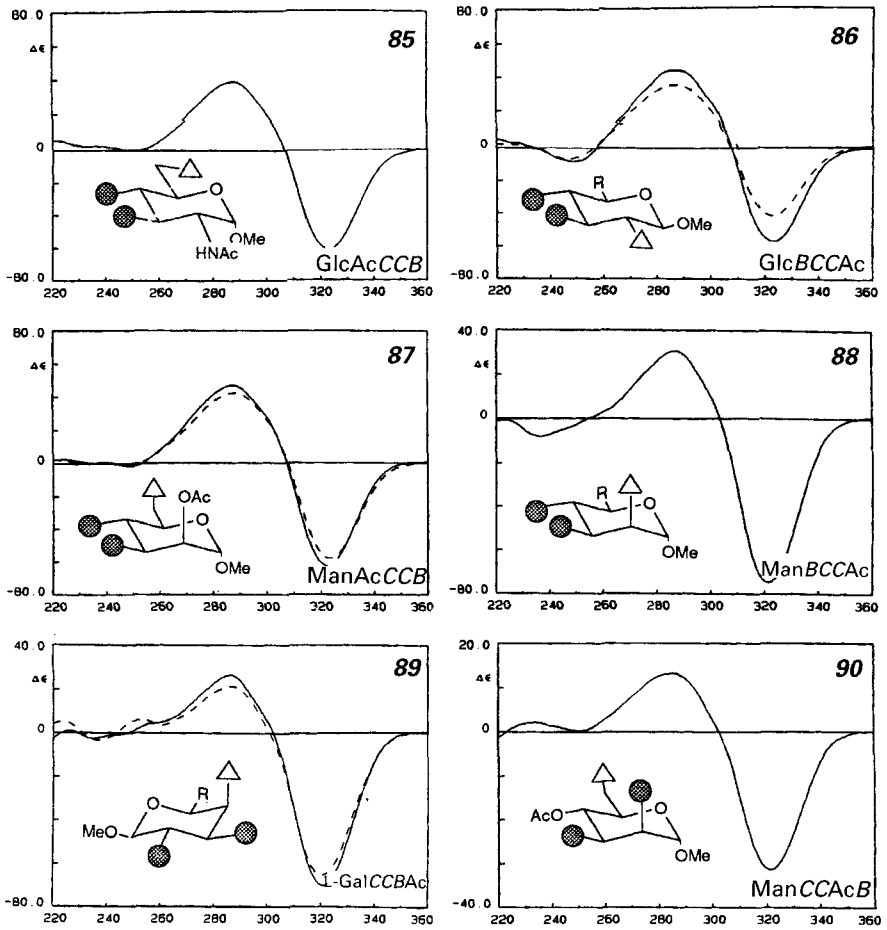


Fig. 18. *CD Spectra of* $BC_2$*-substituted derivatives.*

*85*) Calc.: 288 (+39), 323 (−61).

*86*) D-Xyl*pBCC* (R = H) or D-Qui*BCC* (R = Me); calc.: 249 (−8), 287 (+44), 323 (−56); found for *β*-D-Xyl*BCC*: 247 (−6.7), 287 –(+35.0), 323 (−40.4).

*87*) Calc.: 287 (+47), 322 (−62); found for α-D-anomer: 288 (+42.3), 323 (−58.1).

*88*) *d*-Rha*BCC* (R = Me); calc.: 236 (−8), 287 (+31), 321 (−75).

*89*) L-Fu*CCB* (R = Me) or D-Ara*pCCB* (R = H); calc.: 286 (+27), 321 (−70); found for *β*-L-Fuc*CCB*: 253 (+6.0), 287 (+21.5), 320 (−65).

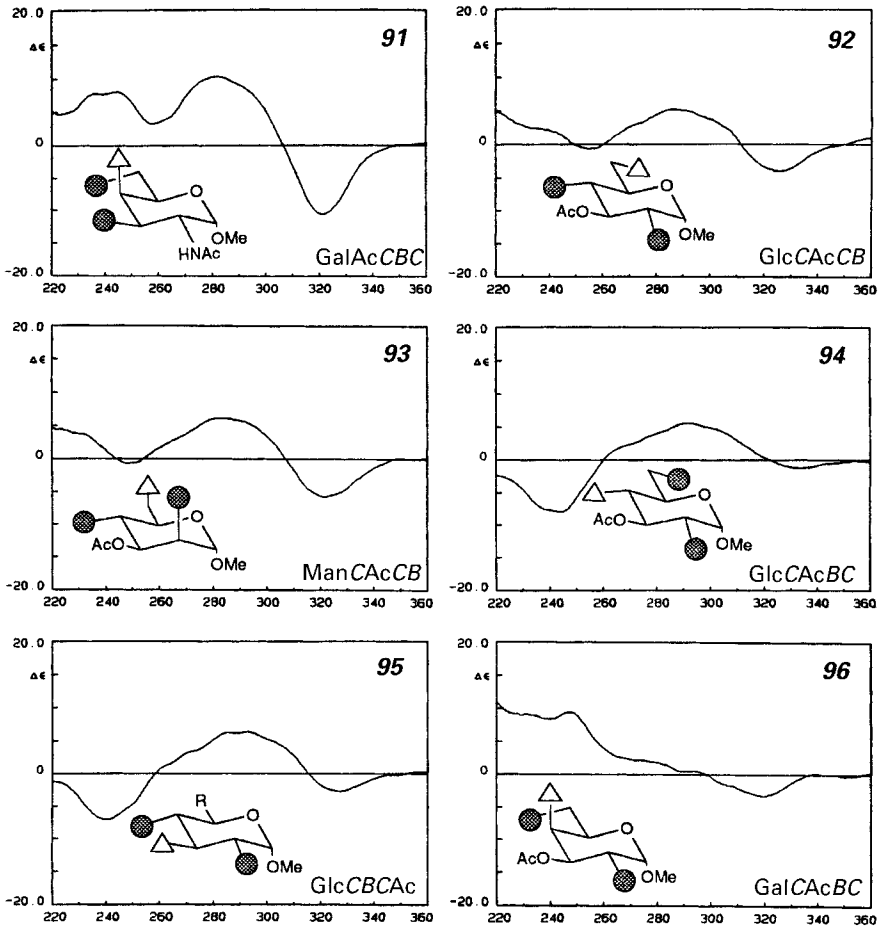


Fig. 19. *CD Spectra of* $BC_2$*-substituted derivatives* (continued).

*90*) Calc.: 233 (+2), 285 (+13), 321 (−31).

*91*) Calc.: 244 (+8), 282 (+10), 321 (−11).

*92*) Calc.: 285 (+5), 326 (−4).

*93*) Calc.: 282 (+6), 322 (−6).

*94*) Calc.: 244 (−8), 283 (sh, +4), 291 (+6), 332 (−1).

*95*) D-Xyl*pCBC* (R = H) or D-Qui*CBC* (R = Me); calc.: 240 (−7), 285 (+6), 293 (+6), 327 (−3).

*96*) Calc.: 247 (+9), 283 (sh, +2), 308 (sh, −2), 319 (−3).

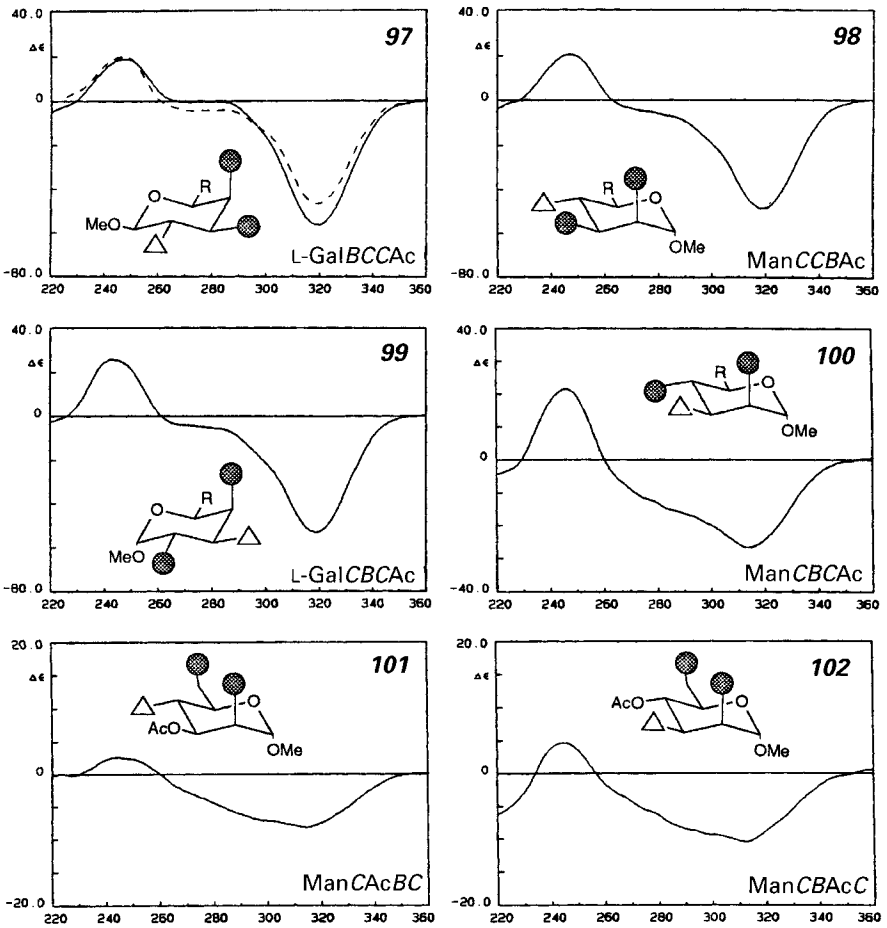


Fig. 20. *CD Spectra of* $BC_2$*-substituted derivatives* (continued).

*97*) L-Fuc*BCC* (R = Me) or D-Ara*pBCC* (R = H); calc.: 247 (+19), 319 (−56); found for *β*-L-Fuc*BCC*: 247 (+19.8), 319 (−46.6).

*98*) D-Rha*CCB* (R = Me); calc.: 247 (+20), 319 (−49).

*99*) L-Fuc*CBC* (R = Me) or D-Ara*pCBC* (R = H); calc.: 243 (+26), 319 (−53).

*100*) D-Rha*CBC* (R = Me); calc.: 246 (+21), 314 (−27).

*101*) Calc.: 244 (+3), 298 (sh, −7), 314 (−8).

*102*) Calc.: 245 (+5), 280 (sh, −6), 299 (sh, −9), 312 (−10).

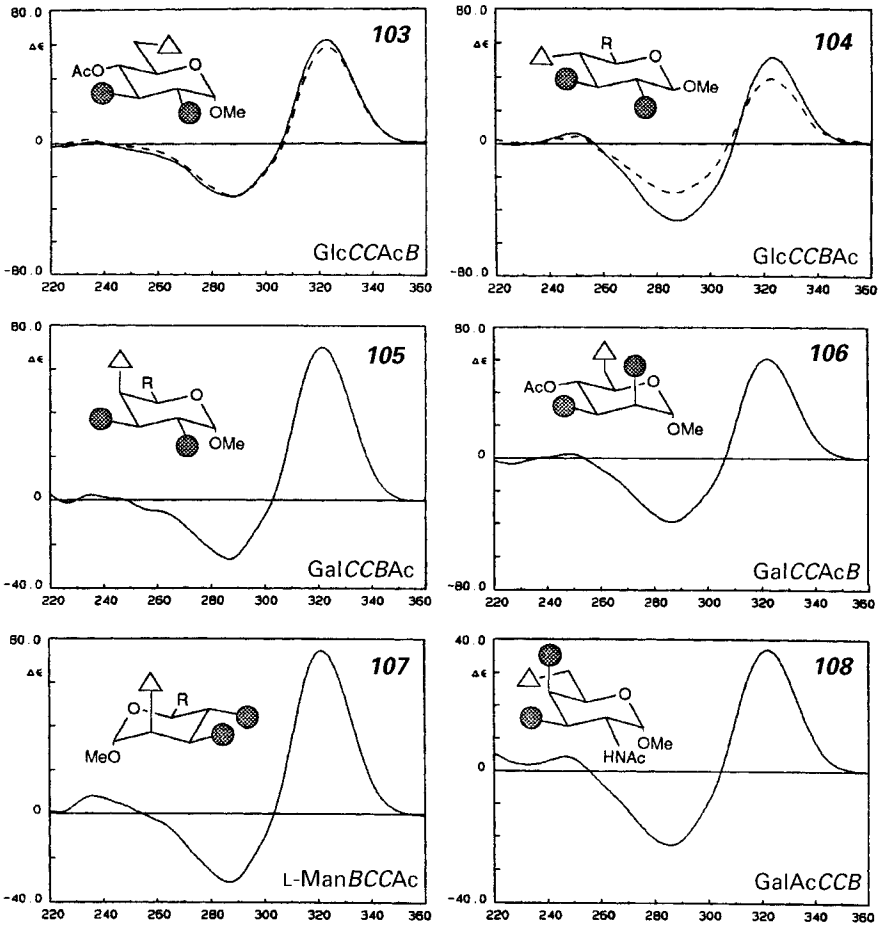


Fig. 21. *CD Spectra of* $BC_2$*-substituted derivatives* (continued).

*103*) Calc.: 287 (−32), 323 (+62); found for α-D-anomer: 288 (−32), 323 (+57.6).

*104*) D-Xyl*pCCB* (R = H) or D-Qui*CCB* (R = Me); calc.: 249 (+6), 288 (−46), 323 (+51); found for β-D-Xyl*CCB*: 250 (+4), 287 (−29.6), 323 (+38.8).

*105*) D-Fuc*CCB* (R = Me) or L-Ara*pCCB* (R = H); calc.: 286 (−27), 321 (+70); found: see *Spectrum 89*.

*106*) Calc.: 287 (−39), 322 (+61).

*107*) L-Rha*BCC* (R = Me); calc.: 236 (+8), 287 (−31), 322 (+75).

*108*) Calc.: 246 (+4), 285 (−22), 322 (+37).

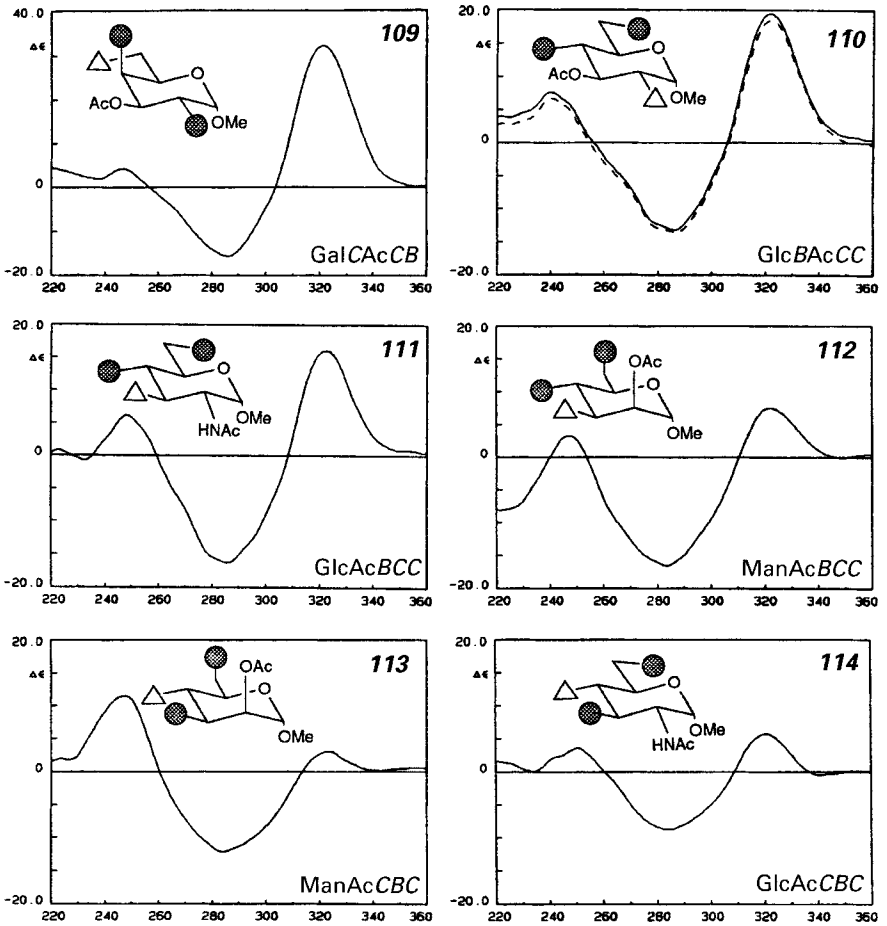


Fig. 22. *CD Spectra of* $BC_2$*-substituted derivatives* (continued).

*109*) Calc.: 247 (+4), 286 (−16), 321 (+32).

*110*) Calc.: 240 (+8), 286 (−13), 321 (+20); found for α-D-anomer: 241 (+6.7), 279 (sh, −12.7), 287 (−13.4), 322 (+18.5).

*111*) Calc.: 248 (+6), 285 (−16), 322 (+16).

*112*) Calc.: 247 (+3), 283 (−16), 321 (+8).

*113*) Calc.: 247 (+12), 284 (−12), 324 (+3).

*114*) Calc.: 250 (+4), 284 (−9), 321 (+6).

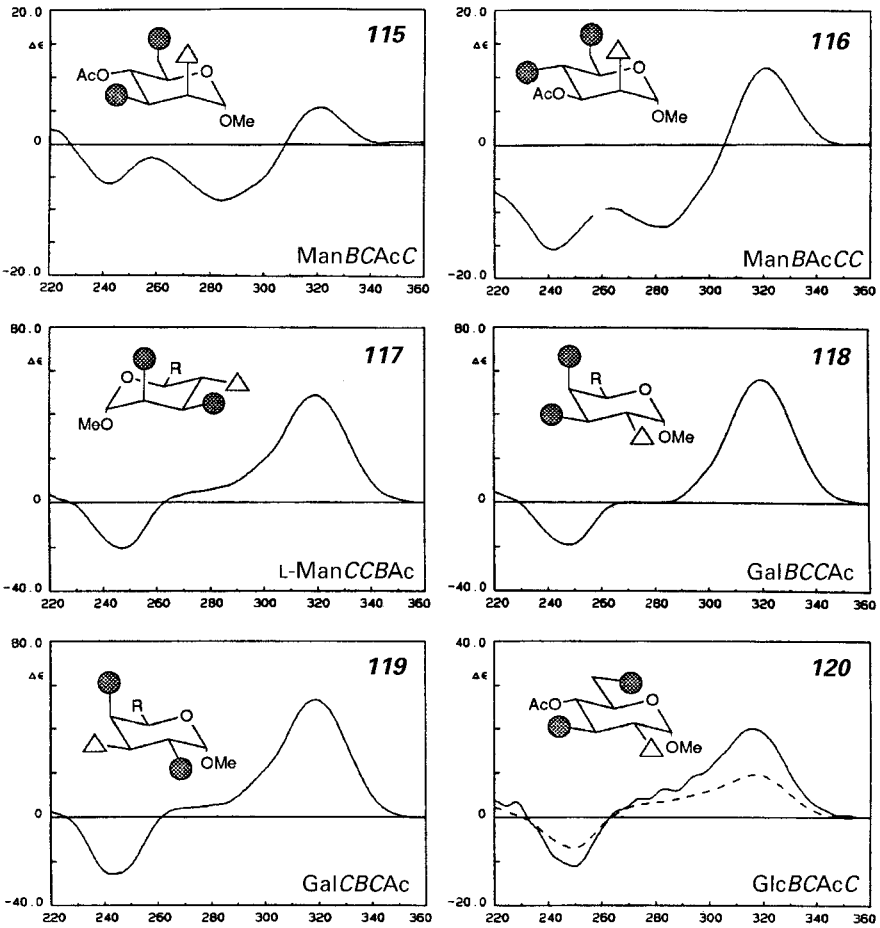


Fig. 23. *CD Spectra of* $BC_2$*-substituted derivatives* (continued).

*115*) Calc.: 242 (−6), 284 (−9), 321 (+5).

*116*) Calc.: 242 (−16), 283 (−12), 320 (+11).

*117*) L-Rha*CCB* (R = Me); calc.: 247 (−20), 319 (+49).

*118*) D-Fuc*BCC* (R = Me) or L-Ara*pBCC* (R = H); calc.: 247 (−19), 319 (+56); found: see *Spectrum 97*.

*119*) D-Fuc*CBC* (R = Me) or L-Ara*pCBC* (R = H); calc.: 243 (−26), 319 (+53).

*120*) Calc.: 250 (−11), 284 (sh, +6), 295 (sh, +9), 316 (+20); found for α-D-anomer: 250 (−7.0), 280 (+3.4), 317 (+9.6).

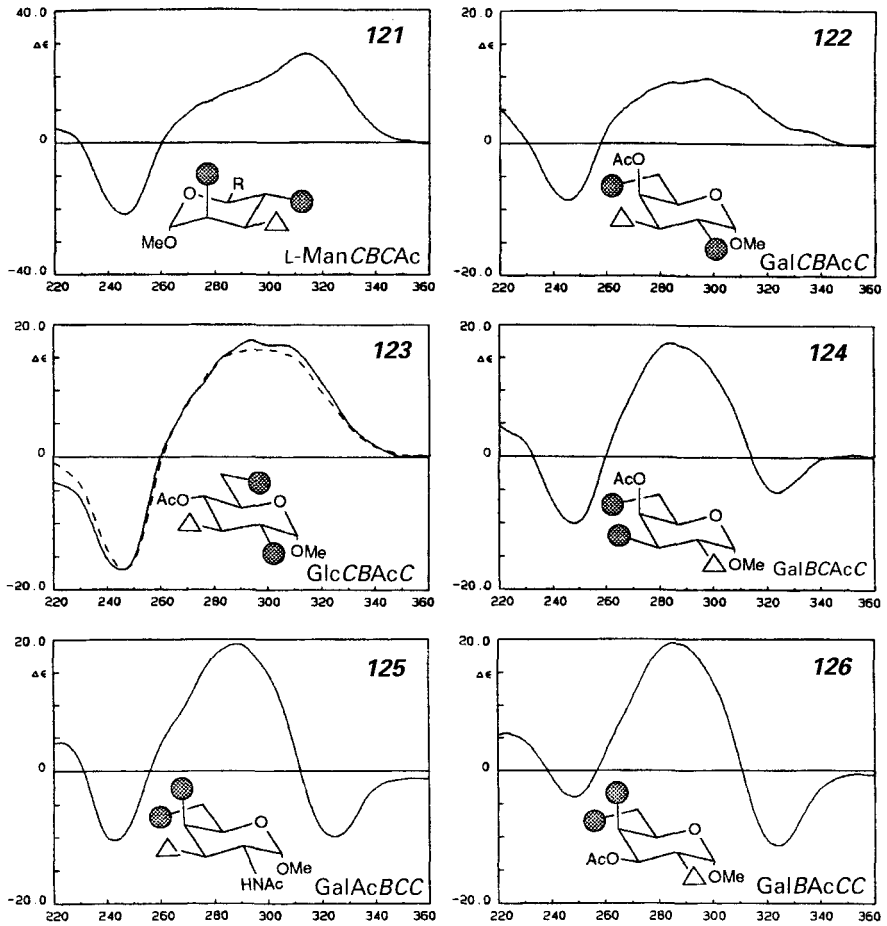


Fig. 24. *CD Spectra of* $BC_2$*-substituted derivatives* (continued).
*121*) L-Rha*CBC* (R = Me); calc.: 246 (−21), 314 (+27).
*122*) Calc.: 245 (−9), 284 (sh, +9), 299 (+10), 311 (sh, +7).
*123*) Calc.: 245 (−17), 294 (+18), 307 (sh, +17); found for α-D-anomer: 246 (−16.7), 297 (+16.2).
*124*) Calc.: 248 (−10), 284 (+17), 323 (−5).
*125*) Calc.: 243 (−10), 289 (+19), 324 (−10).
*126*) Calc.: 249 (−4), 286 (+19), 324 (−11).

## Experimental Part

*General.* All solvents and reagents were prepared or purified as follows: $CH_2Cl_2$ and pyridine were distilled over $CaH_2$, and DMAP was recrystallized from hexane/benzene. $CHCl_3$ was dried by passing through a pipet column of neutral $Al_2O_3$, and MeOH was distilled over $Mg(OMe)_2$. HPLC-grade AcOEt and hexane were used without distillation. The reagent 4-bromobenzoyl chloride (4-BrBzCl) was prepurified by dilution with hexane/$CHCl_3$ 5:1, followed by filtration and concentration under reduced pressure. The reagent 4-methoxycinnamoyl chloride (4-MeOCnCl) was prepared from the acid and thionyl chloride (1.2 equiv.) in refluxing benzene (2 h). Benzene and excess reagent were evaporated, and distillation in a sublimation apparatus (140°/0.1 Torr) afforded pure 4-MeOCnCl. All silver salts were dried *in vacuo* prior to use. All cleavage reactions were performed in special glass tubes (1.1- or 3.3-ml capacity) fitted with *Teflon* screw caps to confine HBr during the reactions *(Fig. 1a)*. The vessels were easily constructed from a glass flow control valve by sealing off the tubing with a flame. Optimization of cleavage conditions by varying reagent ratios, time, and temperature for sugar peracylates was monitored by HPLC after the methyl glycosidation step and methoxycinnamoylation step, and in some cases after the deprotection step. Product mixtures of each step of the oligosaccharide conversions were checked by anal. TLC, and prior to measurements of UV, CD, and MS, all compounds were purified by HPLC. In cases where sufficient amounts of cleavage products (glycosyl bromides, methyl glycosides) were obtained (*e.g.*, those derived from lactose per(4-bromobenzoate)), structures were determined by $^1$H-NMR as either mixtures or purified components obtained from $SiO_2$ chromatography.

Anal. TLC: silica gel *GHLF*/plates *(Analtech)*. HPLC: *Hypersil* 3 μm (4.6 mm × 150 mm) anal. column; UV detection at $\lambda$ 254 nm; isocratic or gradient elution with AcOEt/hexane mixtures (see *Figs. 1* and *2*). UV and CD measurements: MeCN solns., $0.5–1.5 \cdot 10^{-5}$ M; concentrations for bichromophoric derivatives were determined by UV using the experimentally determined average 4-methoxycinnamate $\varepsilon$ values at 311 nm (where 4-bromobenzoates are transparent), *i.e.* $\varepsilon$ = 24000, 45000, and 68000 for mono-, bis-, and tris(4-methoxycinnamates) [11], and average 4-bromobenzoate $\varepsilon$ values at 244 nm, *i.e.*, $\varepsilon$ = 19500, 38200, 57200, and 76400, respectively, for mono-, bis-, tris-, and tetrakis(4-bromobenzoate) [18]; UV spectra, *Perkin Elmer 320 UV* spectrophotometer; CD spectra, *Jasco 500A* spectropolarimeter driven by a *Jasco DP500N* data processor (4 scans were taken of each compound from 200 to 400 nm); after normalization of the CD spectra to $1.0 \cdot 10^{-5}$ M, smoothing and other manipulations were carried out using software developed in house (DFT ( = discrete *Fourier* transform) or FIR ( = finite-duration impulse response filter) procedure for smoothing)[19]. $^1$H-NMR: *Bruker WM 250*, 250 MHz, in $CDCl_3$. MS: *Jeol* instrument; EI or FAB, the latter employing 3-nitrobenzyl alcohol as matrix.

1. *Perbromobenzoylation of Hexopyranose, Deoxysugars, and Aminodeoxysugars (General Procedure)*. Unsubstituted saccharides were first dried *in vacuo* at r.t. overnight. To a soln. of the saccharide in dry pyridine (1 ml for each 10 mg of saccharide) was placed a catalytic amount (*ca.* 0.1 equiv.) of 4-(dimethylamino)pyridine (DMAP) and dry AgOTf (3 equiv./OH), followed by 4-BrBzCl (3 equiv./OH). After stirring at r.t. for 12 h in the dark under Ar, $H_2O$ (one drop/10 mg of starting sugar) was added and the mixture stirred for an additional h. The mixture was then diluted with benzene, and insoluble materials were removed by filtration and washed with benzene. The filtrate and washings were evaporated, suspended in hexane/AcOEt 2:1, and passed over a *Pasteur* pipet filled with a slurry of neutral $Al_2O_3$ (act. II, 1 g/10 mg of starting saccharide) in hexane/AcOEt 2:1. The $Al_2O_3$ column was washed with AcOEt (5 ml/1 g of $Al_2O_3$), the eluate evaporated, and the crude product purified by prep. TLC ($SiO_2$, hexane/AcOEt 2:1). The purified product was dissolved in benzene, frozen with a dry ice/acetone bath, and then kept *in vacuo* for 1 h to afford a white powder suitable for cleavage reactions. TLC: $R_f$ values estimated after UV detection.

*α-Lactose Octakis(4-bromobenzoate)*. Perbromobenzoylation of the sugar with 4-BrBzCl/AgOTf (13 equiv.) afforded a single zone ($R_f \approx 0.4$, $C_6H_6$/AcOEt 3:2), isolated by prep. TLC. $^1$H-NMR (250 MHz, $CDCl_3$): 7.84–7.26 (*m*, 32 H); 6.08 (*d*, *J* = 8.0, H–C(1)); 5.86 (*dd*, *J* = 8.8, 9.5, H–C(3)); 5.69 (*dd*, *J* = 3.2, 5.2, H–C(4′)); 5.67–5.60 (*m*, H–C(2), H–C(2′)); 5.37 (*dd*, *J* = 3.2, 10.4, H–C(3′)); 4.87 (*d*, *J* = 7.8, H–C(1′)); 4.52–4.49 (*m*, 2 H); 4.23 (*dd*, *J* = 9.5, 9.1, H–C(4)); 4.07–4.04 (*m*, H–C(5)); 3.93 (*m*, 2 H); 3.80–3.72 (*dd*, 1 H).

*Digitonin Heptadeca(4-bromobenzoate)*. A commercial sample of digitonin *(Aldrich)* containing several components by TLC was first purified as follows: *i*) $Ac_2O$/pyridine, r.t., 5 h; *ii*) $SiO_2$ chromatography; *iii*) $K_2CO_3$, MeOH, r.t., 4.5 h. Perbromobenzoylation of the purified digitonin (9.8 mg, 8.0 μmol) *without AgOTf* afforded a single zone ($R_f \approx 0.5$; 25 mg, 62%), isolated by prep. TLC (hexane/AcOEt 2:1). $^1$H-NMR (250 MHz, $CDCl_3$):

[19]) *P. Zhou* and *N. Berova*, to be published. Software as well as all data bases are available upon request.

7.96–7.25 (*m*, 66 H); 6.90–6.85 (*m*, 2 H); 5.82–5.20 (*m*, 12 H); 4.96–4.82 (2 H); 4.75–3.88 (20 H); 3.85–3.28 (10 H); 3.10–2.95 (*m*, 1 H); 2.20–0.60 (30 H).

*Sarasinoside $C_1$ Undecakis(4-bromobenzoate)*. Perbromobenzoylation of the sugar (4.1 mg, 3.6 μmol; kindly provided by *I. Kitagawa*) with 4-BrBzCl/AgOTf (4.3 equiv./OH) afforded a single zone ($R_f \approx 0.7$; 8.9 mg, 90%), isolated by prep. TLC. $^1$H-NMR (250 MHz, $CDCl_3$): 7.95–7.30 (42 H); 7.10–6.93 (2 H); 6.12–5.08 (12 H); 4.81–4.68 (1 H); 4.46–3.53 (15 H); 3.32–2.88 (3 H); 2.59–2.42 (*m*, 1 H); 2.40–0.58 (45 H). FAB-MS (3-nitrobenzyl alcohol): 3135 (1.1, $[M + K]^+$).

2. *Trifluoroacetolysis/Bromination and Subsequent Conversions* (see *Scheme 2*). 2.1. *Glycosidic Cleavage*. To a soln. of per(4-bromobenzoate) (*ca.* 1 mg) in $(CF_3CO)_2O$ (130 μl, 0.92 mmol) and oxalyl bromide (79 μl, 0.85 mmol) in a glass tube (stirring bar, septum) under Ar was added, at −78°, 48% HBr soln. (41 μl, 0.36 mmol HBr and 1.76 mmol $H_2O$) *via* syringe (a *Teflon* tube connected to the syringe needle was used such that no contact of aq. HBr soln. with the needle accurred). The glass tube was immediately sealed (hand tight) with the *Teflon* screw cap and heated with an oil bath to 100° for 30–45 min. Afterwards, the hot glass vessel was immersed in a dry ice/acetone bath until a frozen mass was observed, then the screw cap was removed *carefully* (HBr gas is released when the seal is broken). The screw cap was replaced with a rubber septum, and the mixture was placed under an aspirator vacuum, fitted with a drying tube ($CaCl_2$), for 5 min to remove $CF_3COOH$ and other gases (box in *Scheme 2*). The residue was freeze-dried with benzene to give a pale yellow powder which was converted to methyl glycosides.

2.2. *Methyl Glycosidation of Cleavage Products (Glycosyl Bromides)*. In the same glass tube, the powder (see *2.1*) was dissolved in MeOH/$CHCl_3$ 2:3 (0.5 ml) and stirred with $Ag_2O$ (10 mg) at r.t. for 1 h in the dark. After completion of the reaction, the mixture was evaporated, suspended in hexane/AcOEt 1:1, and passed through a *Pasteur*-pipet column (0.5 g of $SiO_2$). The eluate was concentrated and lyophilized with benzene (0.2 ml) to give a powder. An aliquot was dissolved in hexane/AcOEt 3:1 and purified by HPLC for subsequent UV/CD analysis.

The above procedure was carried out on lactose octakis(4-bromobenzoate) in a sufficient quantity to allow for $^1$H-NMR characterization of the products (Glc*BBOB* and Gal*BBBB*). These were found to be identical to authentic samples prepared synthetically.

*Methyl β-D-Glucopyranoside 2,3,6-Tris(4-bromobenzoate)* (Glc*BBOB*). $^1$H-NMR (250 MHz, $CDCl_3$): 8.00–7.48 (*m*, 12 H); 5.43 (*dd*, H–C(3)); 5.34 (*dd*, H–C(2)); 4.82 (*dd*, H–C(6)); 4.63 (*d*, H–C(1)); 4.62 (*dd*, H–C(6′)); 3.82 (*ddt*, H–C(5)); 3.80 (*m*, H–C(4)); 3.53 (*s*, MeO); 3.33 (br. *d*, OH–C(4)).

*Methyl β-D-Galactopyranoside 2,3,4,6-Tetrakis(4-bromobenzoate)* (Gal*BBBB*). $^1$H-NMR (250 MHz, $CDCl_3$): 7.92–7.77 (*m*, 6 H); 7.63–7.49 (*m*, 8 H); 7.40–4.39 (*m*, 2 H); 5.91 (*d*, H–C(4)); 5.69 (*dd*, $J$ = 10.5, 7.9, H–C(2)); 5.53 (*dd*, $J$ = 10.5, 3.4, H–C(8)); 4.71 (*d*, $J$ = 7.9, H–C(1)); 4.66 (*m*, 1 H); 4.41–4.26 (*m*, 2 H); 3.57 (*s*, MeO).

2.3. *4-Methoxycinnamoylation*. To a soln. of the powder (see *2.2*), AgOTf (10 mg), and DMAP (2 mg) in pyridine/$CH_2Cl_2$ (0.1/0.9 ml) was added 4-MeOCnCl (10 mg) under Ar, and the mixture was stirred at r.t. for 4 h in the dark. After adding a drop of $H_2O$ and pyridine (0.5 ml), the mixture was stirred for an additional h, then evaporated, suspended in hexane/AcOEt 2:1, and passed through a *Pasteur*-pipet column (1 g of neutral $Al_2O_3$, act. II). The column was washed with the same solvent and the eluate concentrated to give an oil which was purified by HPLC and analyzed by UV/CD.

3. *Bromoacetolysis/Bromination and Subsequent Conversions* (see *Scheme 3*). 3.1. *General Procedure* (see *General Part, Chapt. 2.2.1, 2.2.2.2*, and *2.2.3*). 3.1.1. *Glycosidic Cleavage and Methyl Glycosydation*. To the oligosaccharide per(bromobenzoate) (200–400 μg) in a glass tube (1.1-ml capacity; stirring bar, septum) under Ar was added $BrCH_2COBr$ (83 μl) *via* syringe. The soln. was cooled to 0° and then $H_2O$ (17 μl) added *via* syringe (*Teflon* tube on the needle tip for delivery of aq. HBr soln.). A *Teflon* spindle valve was used to seal the tube, and the reaction proceeded at the times and temp. described *(vide infra)*. The mixture was then cooled to −78° and the seal broken carefully (HBr gas released); the tube was immediately fitted with a septum and placed under an aspirator vacuum (5 min), followed by placement under high vacuum (30 min).

To the solid residue containing $BrCH_2COOH$ was added dry MeOH (0.2 ml) under Ar at 0°. Then, AgOAc (5 mg) or AgOTf/TMU (8 mg/5 μl) was added with stirring for 1 h in the dark. Silver salts were removed by filtration, the filtrate was concentrated, and the residue, which was suspended in hexane/AcOEt 2:1, was passed through a *Pasteur*-pipet column (slurry of neutral $Al_2O_3$ (act. II) in hexane/AcOEt 2:1). The column was washed with AcOEt (5 ml), and the eluate and washings were evaporated to give a residue which was lyophilized with benzene (0.2 ml). An aliquot can be removed for HPLC analysis.

3.1.2. *Deprotection/4-Methoxycinnamoylation*. To a soln. of the product mixture (see *3.1.1*) in MeOH (0.3 ml) was added thiourea (3 mg), and the mixture was stirred at r.t. for 2 h. $AgNO_3$ (10 mg) in MeCN (0.5 ml) was then added with stirring for an additional 5 min to precipitate the thiourea. The mixture was diluted with $CH_2Cl_2$ (3 ml)

and passed over a *Pasteur*-pipet column filled with $SiO_2$ (0.5 g). The column was washed with $CH_2Cl_2$/MeOH 9:1 (10 ml), and the eluate and washings were evaporated and then lyophilized with benzene (0.2 ml) to give an amorphous powder. An aliquot can be removed for HPLC analysis.

To a soln. of the product in pyridine (0.2 ml) was added AgOTf (5 mg), 4-MeOCnCl (5 mg), and DMAP (cat.) under Ar. The reaction proceeded at r.t. for 12 h in the dark, then $H_2O$ (one drop) was added and the mixture stirred for an additional h. The mixture was evaporated, suspended in hexane/AcOEt 2:1, then passed through a *Pasteur*-pipet column filled with 1 g of neutral $Al_2O_3$ slurry (act. II) in hexane/AcOEt 2:1. The column was washed with AcOEt (5 ml), and the eluate and washings were evaporated to afford a residue which was HPLC-purified. Purified products were isolated and analyzed by UV, CD, and MS.

3.2. *Digitonin Heptadecakis(4-bromobenzoate)* (see *Scheme 4*). As described in the *General Part*, the earlier version of oligosaccharide conversion (see *Chapt. 2.2.1, 2.2.2.1,* and *2.2.3*) was applied to digitonin [15].

3.2.1. *Glycosidic Cleavage and Methyl Glycosydation.* Under Ar, $BrCH_2COBr$ (250 µl, 2.87 mmol) and $H_2O$ (50 µl, 2.78 mmol) were added to digitonin heptadecakis(4-bromobenzoate) (2.1 mg, 0.42 µmol) in a glass tube (3.3-ml capacity, septum) at −78°. After sealing the vessel with the *Teflon* cap, the mixture was stirred at 60° for 12 h in an oil bath. The mixture was again cooled to −78° and the *Teflon* valve carefully opened. HBr gas was removed *in vacuo* under aspirator pressure (5 min) and then under high vacuum (30 min). The resulting solid was dissolved in 10 ml of cold hexane/AcOEt 3:1 and washed with cold sat. $NaHCO_3$ soln. (2 × 5 ml), followed by cold $H_2O$ (2 ml). The org. layer was dried ($MgSO_4$), filtered, and evaporated. The residue was freeze-dried with benzene (0.3 ml) *in vacuo* for 1 h to give a white, amorphous powder.

One third of the powder (corresponding to 140 nmol of digitonin perbromobenzoate) was dissolved in MeOH/$CHCl_3$ 1:2 (0.6 ml) under Ar, then $Ag_2CO_3$ (12 mg) and AgOTf (6 mg) were added, and the mixture was stirred at r.t. for 1 h in the dark. The mixture was evaporated and the residue suspended in 1 ml of hexane/AcOEt 3:1, and passed over a *Pasteur*-pipet column filled with a slurry of $SiO_2$ (0.4 g) in hexane/AcOEt 3:1. The $SiO_2$ column was washed with 5 ml of hexane/AcOEt 3:1 and the eluate concentrated to give an oily material.

3.2.2. *Deprotection/4-Methoxycinnamoylation.* To a soln. of the methyl glycoside mixture in $CHCl_3$/MeOH 2:1 (0.6 ml) was added $NaHCO_3$ (2 mg) and thiourea (2 mg), and the mixture was stirred at 25° for 2 h. After evaporation, the residue was suspended in hexane/AcOEt 2:3 and passed over a *Pasteur*-pipet column filled with a slurry of $SiO_2$ (0.4 g) in hexane/AcOEt 3:1. The column was washed with 10 ml of hexane/AcOEt 2:3, and the eluate and washings were evaporated. The resulting residue was lyophilized with benzene (0.3 ml) as previously described to afford a white powder.

To a soln. of the product mixture in 0.5 ml of dry pyridine/$CH_2Cl_2$ 1:4 were added AgOTf, DMAP, and 4-MeOCnCl (9 mg) under Ar. The mixture was stirred at r.t. for 5 h in the dark. A drop of $H_2O$ and pyridine (0.5 ml) were added, and the mixture was stirred for an additional h. After evaporation, the residue was suspended in hexane/AcOEt 3:1 and passed over a *Pasteur*-pipet column filled with a slurry of $Al_2O_3$ (act. II, 1 g) in hexane/AcOEt 3:1. The column was washed with 10 ml of hexane/AcOEt 3:1, and the eluate and washings were evaporated to afford a colorless oil which was analyzed by HPLC, UV, and CD.

The above procedures *(Exper. 3.2)* have been carried out with 70 nmol of digitonin per(bromobenzoate) with the same results [15], and the more general procedure (see *Exper. 3.1*) yielded equally satisfactory results.

3.3. *Sarasinoside $C_1$ Undecakis(4-bromobenzoate)* (see *Scheme 5*). To the sugar per(4-bromobenzoate) (260 µg, 95 nmol) were added $BrCH_2COBr$ (83 µl) and $H_2O$ (17 µl), and the mixture was stirred at 50° for 12 h. Then, the mixture of cleavage products was converted to methyl glycosides with AgOTf (8 mg)/TMU (5 µl) in MeOH (200 µl) for 1 h at r.t. (see *Exper. 3.1.1*). Subsequent conversion to bichromophoric derivatives was performed as described in *3.1.2*. FAB-MS (3-nitrobenzyl alcohol): GalN*BBBB*: 926 (100, $[M + H]^+$), 894 (23, $[M - OMe]^+$); GlcN*BBBC*: 904 (46, $[M + H]^+$), 872 (7, $[M - OMe]^+$); GalNAc*BBB*: 824 (7, $[M + K]^+$), 808 (17 $[M + Na]^+$), 786 (47, $[M + H]^+$), 754 (28, $[M - OMe]^+$); GlcNac*BBC*: 762 (62, $[M + H]^+$).

The work described here started with the finding that additivity relations hold in split CD amplitudes (see [18]). The authors are grateful to everyone who has been involved in previous stages of this study. This work was supported by the *National Institutes of Health* grant GM 34509.

## REFERENCES


[1] V. Ginsberg, P. W. Robbins, Eds., 'Biology of Carbohydrates', Wiley, New York, 1984, Vol. 2.
[2] S. B. Mahato, S. K. Sarkar, G. Poddar, *Phytochemistry* **1988,** *27,* 3067.
[3] B. Lindberg, *Chem. Soc. Rev.* **1981,** *10,* 409; C. J. Biermann, G. D. McGinnis, Eds., 'Analysis of Carbohydrates by GLC and MS', CRC Press, Boca Raton, Florida, 1989.
[4] R. Geyer, H. Geyer, S. Kuhnhardt, W. Mink, S. Stirm, *Anal. Biochem.* **1983,** *133,* 197.
[5] K. Nakanishi, M. Kuroyanagi, H. Nambu, E. M. Oltz, R. Takeda, G. L. Verdine, A. Zask, *Pure Appl. Chem.* **1984,** *56,* 1031.
[6] K. Nakanishi, M. H. Park, R. Takeda, J. T. Vasquez, W. T. Wiesler, 'Stereochemistry of Organic and Bioorganic Transformations', Ed. W. Bartmann, Verlag Chemie, Weinheim, 1986, pp. 303–319.
[7] R. Takeda, A. Zask, K. Nakanishi, M. H. Park, *J. Am. Chem. Soc.* **1987,** *109,* 914.
[8] M. H. Park, R. Takeda, K. Nakanishi, *Tetrahedron Lett.* **1987,** *28,* 3823.
[9] M. Chang, H. V. Meyers, K. Nakanishi, M. Ojika, J. H. Park, M. H. Park, R. Takeda, J. T. Vazquez, W. T. Wiesler, *Pure Appl. Chem.* **1989,** *61,* 1193.
[10] W. T. Wiesler, J. T. Vazquez, K. Nakanishi, *J. Am. Chem. Soc.* **1987,** *109,* 5586.
[11] J. T. Vazquez, W. T. Wiesler, K. Nakanishi, *Carbohydr. Res.* **1988,** *176,* 175.
[12] H. V. Meyers, M. Ojika, W. T. Wiesler, K. Nakanishi, *Carbohydr. Res.* **1989,** in press.
[13] N. Harada, K. Nakanishi, 'Circular Dichroic Spectroscopy – Exciton Coupling in Organic Stereochemistry', University Science Books, Mill Valley, CA, 1983.
[14] A. Jeanes, C. A. Wilham, G. E. Hilbert, *J. Am. Chem. Soc.* **1953,** *75,* 3667.
[15] M. Ojika, H. V. Meyers, M. Chang, K. Nakanishi, *J. Am. Chem. Soc.* **1989,** *111,* 8944.
[16] L. Rosenfeld, C. E. Ballou, *Carbohydr. Res.* **1974,** *32,* 287.
[17] C. F. H. Allen, J. A. Van Allan, *Org. Synth., Coll. Vol.* **1955,** *3,* 751; K. Ohno, N. Naruse, H. Takeuchi, *Tetrahedron Lett.* **1979,** *3,* 251.
[18] H. W. Liu, K. Nakanishi, *J. Am. Chem. Soc.* **1982,** *104,* 1178.
[19] J. Golik, H. W. Liu, M. DiNovi, J. Furukawa, K. Nakanishi, *Carbohydr. Res.* **1983,** *118,* 135.